

A SURVEY OF ANT-ASSOCIATED FUNGAL DIVERSITY IN CANOPY  
BROMELIADS FROM THE ECUADORIAN AMAZON

by

Daniel O. Puckett, B.S.

A thesis submitted to the Graduate Council of  
Texas State University in partial fulfillment  
of the requirements for the degree of  
Master of Science  
with a Major in Biology  
December 2018

Committee Members:

David Rodriguez, Chair

Chris Nice

Shawn McCracken

**COPYRIGHT**

By

Daniel O. Puckett

2018

## **FAIR USE AND AUTHOR'S PERMISSION STATEMENT**

### **Fair Use**

This work is protected by the Copyright Laws of the United States (Public Law 94-553, section 107). Consistent with fair use as defined in the Copyright Laws, brief quotations from this material are allowed with proper acknowledgement. Use of this material for financial gain without the author's express written permission is not allowed.

### **Duplication Permission**

As the copyright holder of this work I, Daniel O. Puckett, authorize duplication of this work, in whole or in part, for educational or scholarly purposes only.

## **ACKNOWLEDGEMENTS**

I would like to thank my advisor, Dr. David Rodriguez, for his guidance, expertise, and support throughout my graduate career. I would also like to thank Dr. Shawn McCracken for allowing me to use the specimens and accessory data he collected for this study and for his valuable feedback on my proposal and thesis. I would also like to thank Dr. Chris Nice for his feedback and suggestions on my proposal and thesis. My labmates, Stephen Harding, Carlos Baca, Devlin Jackson, and Mireya Escandon all deserve my thanks for helping me with lab techniques, procedures, sorting specimens, and moral support. Lastly, I thank my family for their support and encouragement throughout my time as a graduate student.

## TABLE OF CONTENTS

	<b>Page</b>
ACKNOWLEDGEMENTS .....	iv
LIST OF TABLES .....	vi
LIST OF FIGURES .....	vii
CHAPTER	
I. INTRODUCTION .....	1
II. METHODS .....	6
III. RESULTS .....	10
IV. DISCUSSION.....	15
APPENDIX SECTION.....	38
LITERATURE CITED.....	39

## LIST OF TABLES

<b>Table</b>	<b>Page</b>
1. List of all fifty-three fungal OTUs and their highest levels of taxonomic classification along with the ant specimens to which they belong . . . . .	21
2. List of all fungal species and genera, their known hosts or substrates, and the relationship to their hosts or substrates . . . . .	23
3. All unknown OTUs along with their highest level of taxonomic classification, their likely next level of taxonomic classification, and the match percentage of the closest genetic sequence of known fungal species with full coverage on GenBank and UNITE fungal databases . . . . .	24

## LIST OF FIGURES

<b>Figure</b>	<b>Page</b>
1. Alpha diversity plot .....	25
2. Average alpha diversity plot per bromeliad .....	26
3. Shannon-Wiener and Simpson plot ..	27
4. Pie chart of phyla .....	28
5. Stacked bar plot of relative fungal abundance .....	29
6. Phylogeny of UF001 .....	30
7. Phylogeny of UF002 .....	31
8. Phylogeny of UF003 .....	32
9. Phylogeny of UF004 .....	33
10. Phylogeny of UF006 .....	34
11. Phylogeny of UF007 .....	35
12. Phylogeny of UF008 .....	36
13. Phylogeny of UF009 .....	37

## I. INTRODUCTION

Fungi are among the most diverse organisms on the planet, yet much is still undiscovered in terms of their abundance, richness, taxonomic relationships, and evolutionary history. The number of known species is at least 120,000, and conservative estimates of species have put their total numbers above 1.5 million, although more recently it is estimated there are 2.2 to 3.8 million species (Hawksworth 2001; Hawksworth and Lücking 2017). Fungi have a vast range of reproductive and survival strategies that enable them to colonize almost all parts of the earth. Many fungi associate with animals in symbiotic relationships, which range from parasitic to commensal to mutualistic. These relationships are under-studied, especially in tropical areas, despite their seeming ubiquity in nature.

Arthropods, and in particular, insects, are common hosts for fungi. Whether they carry fungi inside or outside of their exoskeletons, insects are important for the life cycles of various phyla of fungi, while fungi are also important for the life cycles of various insects. Some parasitic fungi belonging to the Cordycipitaceae and Ophiocordycipitaceae families, such as *Cordyceps sp.* and *Ophiocordyceps sp.*, use insects as hosts to absorb nutrients and release spores in an advantageous manner. These genera are known to alter insect host behavior to climb vegetation and lock themselves in place, which allows the fungal mycelium to grow rapidly within the host and send forth fruiting bodies that burst through the host's exoskeleton to spread spores (Evans et al. 2011). Not all fungi are harmful to insects, and many are even beneficial. Fungal endosymbionts in bark beetles, ambrosia beetles, termites, and ants have been shown to detoxify harmful compounds produced by plants as well as aid in metabolizing compounds such as terpenes, lignin,

tannins, and esters (Dowd 1992). Ants, which have many micro- and macro-fungal symbiotic relationships, have a high diversity and abundance in tropical rainforests, specifically in the canopy layers (Moran and Southwood 1982; Stuntz et al. 2002). Ants have been shown to be the most numerically abundant animal in the upper canopy of forests (Nadkarni 1994), which makes them an ideal host organism for microbiome studies.

Fungal richness has been shown to be highly correlated with proximity to the equator, with tropical regions possessing the highest richness (Tedersoo et al. 2014). The canopy layer of tropical rainforests supports an incredibly diverse range of organisms and boasts some of the highest species richness in the world (Lowman and Schowalter 2012). Bromeliads, which are prevalent epiphytic plants with large water tanks that serve as microhabitats, represent unique microcosms for microorganisms, arthropods, amphibians, and many other organisms in the canopy. Because the communities that inhabit bromeliads are inherently isolated, bromeliads are useful in the study of microbiomes across the landscape. The organisms that live in canopy tank bromeliads are separated not only from the lower forest layers, but from other bromeliad communities in other trees. By taking a molecular approach to identifying ant-associated fungal microbiomes in various tank bromeliads, much can be discovered about how isolated microorganisms evolve, what biotic and abiotic factors influence microbiome diversity, and the structure of populations.

One of the most popular and effective techniques for genetically identifying species is DNA barcoding. This consists of amplifying and sequencing short fragments of typically highly conserved DNA sequences and comparing them to databases of known

sequences (Moritz and Cicero 2004; Hebert et al. 2005). By comparing these experimentally-derived sequences to the sequences of known species, they can be rapidly identified. The amplification step is carried out using polymerase chain reaction (PCR), a technique that allows billions of copies of the DNA sequence to be made using primers that anneal at targeted sites (Mullis and Faloona 1987). Once the DNA has been amplified, these fragments, called amplicons, can be sequenced in many ways. However, when the source DNA in the sample is potentially from multiple species, as would be the case when extracting DNA from gut biomes, more powerful sequencing techniques called Next Generation Sequencing are needed.

Next Generation Sequencing (NGS) is a set of DNA sequencing technologies that allow high throughput analysis of genetic data in parallel (Mardis 2008). NGS has been used to discover surprising numbers of fungi from environmental soil samples (Buée et al. 2009). Because of the parallel and high throughput nature of NGS, it allows one to analyze environmental samples in which many species are present. Thus, it lends itself well to the study of microbiome studies due to the great number of species that can be found within each host. The NGS platform that will be used for this study is Illumina MiSeq sequencing.

Illumina sequencing is a high-throughput NGS platform that allows hundreds of millions of nucleotide reads in a single run (Quail et al. 2008). One of its largest advantages over traditional sequencing is that it can accomplish this in a massively parallel fashion; thus, hundreds of pooled, mixed samples can be uniquely identified all at once in a short amount of time (Smith et al. 2008). Illumina is highly effective for microbiome studies due to its massively parallel capabilities and its speed advantage over

other techniques such as bacterial cloning (Gloor et al. 2010). Although Illumina cannot sequence long contiguous fragments effectively, it is still accurate across genomes with high coverage due to overlapping sequence reads; on the other hand, Illumina is highly effective and accurate for short reads (Liu et al. 2012). Thus, it is evident that rapid identification of fungal microbiome species via Illumina can be accomplished by targeting short informative DNA regions.

The target DNA region for this study is the first internal transcribed spacer (ITS1). ITS has gained popularity as a universal barcode for fungi, as it is broadly informative in differentiating fungal species due to the presence of more interspecific sequence variation than intraspecific sequence variation (Schoch et al. 2012). Barcoded Illumina-specific ITS primers, which allow identification of fungi on an ant-by-ant basis, were used. By using Illumina sequencing to acquire all fungal ITS sequences associated with each ant, the plethora of ant-associated fungal species can be identified, diversity can be assessed, and phylogenies can be constructed.

A major objective of this study is to perform a preliminary survey of the ant-associated fungal diversity in bromeliads in a tropical rainforest. There were multiple questions I wanted to answer via this study. First, what fungi are associated with ants in Amazon rainforest canopy bromeliads? Second, what levels of fungal diversity exist within and among ants? Third, what unknown fungi—either unsequenced or undescribed—are associated with these ants? This exploratory study will provide sequence data that will elucidate the abundance and diversity of the various ant-associated fungi within canopy bromeliads. The comparison of the species found helps uncover a great deal about the evolutionary history of tropical ant-fungi associations and

the current make-up of the populations and communities associated with these canopy bromeliads. This study lays the groundwork for potential conservation efforts in this area that is under threat from climate change, deforestation, and human encroachment. Additionally, this study highlights the vast number of unsequenced, unidentified, and undescribed fungi in this niche.

## II. METHODS

The specimens for this study were collected in a region of tropical rainforest in Amazonian Ecuador in the Yasuní National Park at the Tiputini Biodiversity Station (-0.63461, -76.18410). Bromeliads 20 to 35 meters above the ground in the canopy layer of the forest were cut from the trees at their bases and lowered to the ground while enclosed in plastic bags to prevent spillage. Once on the ground, they were cut open and all contents of the bromeliads were collected. Arthropods were separated out and preserved in 95% ethanol. Ants were then separated out from the other arthropods and preserved in fresh 95% ethanol. At the time of bromeliad collection, various biotic and abiotic conditions were described: coordinates, altitude, tree diameter at breast height, tree height, number of bromeliads on the tree, canopy cover, bromeliad elevation, bromeliad height, bromeliad diameter, bromeliad leaf numbers, bromeliad water volume, temperature and relative humidity at bromeliad, soil pH, soil moisture, water pH, and number of anurans in each bromeliad.

Before DNA extraction, each ant specimen was assigned a unique identifier code and photo vouchers were taken from multiple angles. The ants were washed with 95% ethanol and then dried using lint-free tissues. 2-3 mm<sup>3</sup> sections of each ant's thorax were excised using a sterile scalpel and the excised tissues were put into sterile labeled 1.5 mL Eppendorf tubes. The excised tissues were mechanically sheared by repeatedly crushing with sterile forceps tips. DNA extraction was performed according to the Thermo Fisher Scientific GeneJET Genomic DNA Purification Protocol, with the only deviation from the protocol being tissue incubation in digestion solution for 14 hours at 56°C. DNA was

released from the spin column membrane and suspended in 200  $\mu$ L of elution solution within 1.5 mL Eppendorf tubes, which were then stored at 4° C.

To ensure thorough amplification of the target sequence, a preliminary enrichment step was performed. An approximately 1000 base pair sequence containing the target sequence was first amplified—under a sterile laminar flow hood to prevent foreign fungal contamination—for 96 ant specimens using the V9G (5'-TTACGTCCCTGCCCTTTGTA-3') (Hoog and Ende 1998) and ITS4 (5'-TCCTCCGCsTTATTGATATGC-3') (White et al. 1990) primers. Positive and negative controls were included to verify the integrity of the reactions and to ensure contamination did not occur. The PCR reaction mixtures consisted of 2.5  $\mu$ L of nuclease-free water, 2.5  $\mu$ L of DreamTaq PCR Master Mix (2X) by Thermo Fisher Scientific, 0.50  $\mu$ L of V9G primer (10  $\mu$ M), 0.50  $\mu$ L of reverse ITS4 primer (10  $\mu$ M), and 0.50  $\mu$ L of template DNA solution in elution buffer. Thermal cycling began with a 1-minute incubation step at 94 °C. This was followed by 3 steps repeated for 35 cycles: denaturation at 94 °C for 30 seconds, primer annealing at 52 °C for 30 seconds, and elongation at 68 °C for 30 seconds. Amplification concluded with a 7-minute step at 68 °C. The PCR amplicons were cleaned to remove excess nucleotides and primers by using the ExoSAP protocol by Thermo Fisher Scientific. The purified amplicons were stored at -20° C.

Following enrichment, the ITS1 region was amplified using 96 uniquely barcoded, Illumina-specific ITS2 reverse primers for a parallel run on Illumina MiSeq. The PCR reaction mixtures consisted of 2.5  $\mu$ L of nuclease-free water, 2.5  $\mu$ L of DreamTaq PCR Master Mix (2X) by Thermo Fisher Scientific, 0.50  $\mu$ L of ITS1 (modified from White et al. 1990) forward primer (10  $\mu$ M), 0.50  $\mu$ L of ITS2 (White et al.

1990) reverse primer (10  $\mu$ M), and 0.50  $\mu$ L of enriched PCR products. Thermal cycling began with a 1-minute incubation step at 94 °C. This was followed by 3 steps repeated for 35 cycles: denaturation at 94 °C for 30 seconds, primer annealing at 52 °C for 30 seconds, and elongation at 68 °C for 30 seconds. Amplification concluded with a 7-minute step at 68 °C. The PCR amplicons were cleaned with Agencourt AMPure XP magnetic beads according to the manufacturer's protocol. The purified amplicons were stored at -20° C.

The DNA concentration of each amplicon was quantified using the Qubit™ dsDNA HS Assay Kit by Invitrogen™. To normalize all samples for the Illumina sequencing, 1 ng of DNA from each sample was transferred into a single 2 mL DNA LoBind tube. This pooled library was then cleaned again using magnetic beads according to the manufacturer's protocol. After cleanup, the pooled library was quantified using Qubit™ and then diluted to a 4 nM solution which was stored at -20° C. For Illumina sequencing, the MiSeq Reagent Kit v3 (600-cycle) was used. The library solution was loaded onto the reagent cartridge along with PhiX control v3 (10%), and the library was sequenced according to the manufacturer's protocol using ITS Read 1 sequencing primer (5'-TTGGTCATTTAGAGGAAGTAAAAGTCGTAACAAGGTTTCC-3'), ITS Read 2 sequencing primer (5'-CGTTCTTCATCGATGCVAGARCCAAGAGATC-3'), and index sequencing primer (5'-TCTCGCATCGATGAAGAACGCAGCCG-3').

Illumina sequencing data were demultiplexed into FASTQ files corresponding to each ant sample. The Dada2 package for R (3.4.3) was loaded on an iMac. Using Dada2, the forward reads were filtered and trimmed to 120 base pairs, and error rates were estimated to assess accuracy of the reads. Chimeras were removed, and then identical

sequences were combined and assigned abundance values to improve computation time and prevent redundancy in analyses. All sequence variants were inferred for each sample, and an OTU (Operation Taxonomic Unit) table containing all fungal sequence variants and their corresponding ant sample was constructed. Taxonomic classification was performed on this sequence variant table by referencing the UNITE ITS fungal database (Kõljalg et al. 2013).

Diversity and species evenness were analyzed with R (3.4.3) using the Phyloseq (3.7) package. Alpha diversity was plotted using the Phyloseq (3.7) package in R for each ant specimen as well as for each bromeliad. A pie chart was constructed with R (3.4.3) showing the proportion of fungal sequences belonging to each phylum as well as the OTUs unidentified to genus level within each phylum. Using Phyloseq (3.7), a diversity plot using the Shannon-Wiener diversity index was constructed for all 47 ant specimens and their respective fungal microbiomes. A diversity plot using the Simpson evenness index was also constructed for all 47 ant specimens and their respective fungal microbiomes.

To assess relatedness to known taxa and potentially narrow down likely taxonomy of the fungal unknowns, the ten most similar fungal ITS1 sequences to each unknown taxon in this study were downloaded from GenBank. These sequences were aligned using MUSCLE within Geneious 9.1.8 (<http://www.geneious.com>, Kearse et al., 2012) with default settings. The 120 base pair alignments were used to generate unrooted Neighbor Joining phylogenetic trees using PAUP 4b10 in Geneious. The nucleotide substitution model was selected using ModelTest with AIC, and the General Time Reversible model with invariant sites and gamma distribution was selected for each tree generated.

### III. RESULTS

Successful fungal sequencing occurred for forty-seven ant specimens with 63,968 reads via Illumina MiSeq. Within these forty-seven ants, fifty-three total unique fungal sequences were observed. A list of unique sequence variants and their highest assigned taxonomy is shown in Table 1. Fungi belonging to the phylum Ascomycota made up 93.55% of the sequence reads covering forty-five OTUs, while those belonging to the phylum Basidiomycota made up 6.45% of the sequence reads covering eight OTUs. Eight out of the forty-five Ascomycete OTUs were unable to be identified to genus, while only one out of the eight Basidiomycete OTUs was unable to be identified to genus (Figure 4).

Of the sequences that were identified, *Cladosporium* was the most frequently identified genus with six representative sequence variants (Table 1). The next most represented genera were *Mycosphaerella* and *Ramularia* with three sequence variants each (Table 1). Twenty-three of the sequences were unable to be identified to species, nine were unable to be identified to genus, five were unable to be identified to family, three were unable to be identified to order, and one was unable to be identified to class.

Fungal alpha diversity was low for most ants with an average of 1.829 fungal species per ant. The highest alpha diversity seen was 6, which occurred for only two ant specimens, DPB001 and DPB002 (Figure 1). The lowest alpha diversity seen was in ants that only had one fungal sequence, which occurred for twenty-three ants. The average alpha diversities for ants collected from each bromeliad are shown in Figure 2. Bromeliad BLKT01-B04 has the highest average fungal alpha diversity with 5, while bromeliads BLKT02-B05, LAGT01-B05, LAGT02-B03, PHT01-B03, and PHT02-B04 all have average alpha diversities of 1 (Figure 2). Ants collected from the BLK region have a

higher average alpha diversity than those collected from the LAG and PH regions within the study site. Those averages are 2.33, 1.375, and 1.615 respectively.

The diversity plotted using the Shannon-Wiener diversity index shows that there are stark differences between the ants with both low diversity and read numbers compared to ants with both higher diversity and read numbers (Figure 3). The two ants with the highest diversity using the Shannon-Wiener diversity index were DPB001 and DPB002, which were the ants with the highest uncorrected alpha diversities (Figure 1). The twenty-three ants that contained only one unique fungal sequence were assigned alpha diversity measures of 0 under the Shannon-Wiener index, as diversity for singletons cannot be positive. The Simpson evenness index plot, also seen in Figure 3, shows very similar results for the ants when compared to the Shannon-Wiener plot. Again, DPB001 and DPB002, which each had six unique fungal sequences, had the highest diversity measures when using the Simpson algorithm. Just as before, the twenty-three singletons have measures of 0. All ants, with the exception of DPB061, had the same diversity measures relative to each other using these two indices. DPB061 had different diversity measures compared to other ants between the Shannon-Wiener and Simpson plots due to the presence of multiple low-abundance sequences and one high abundance sequence.

The relative abundance of fungal genera in each ant specimen is shown in a stacked bar plot (Figure 5). These abundances are based on read numbers of the unique sequences. The legend differentiates the genera, and the OTUs unable to be identified to genus level are shown as grey bars and labeled as “Unknown.”

Fungal sequences that were unidentified to at least the level of genus were given additional unique voucher ID numbers, and those are listed in Table 2 along with their highest level of taxonomic placement and the closest genetic match with a known fungal species. The fungal sequences that were of uncertain taxonomic placement were placed into Neighbor Joining phylogenetic trees with their closest genetic matches for the full 120 base pair sequences. The phylogenetic trees generated are shown in Figures 6 to 13. The trees are color-coded at the tip labels to differentiate different taxa within the respective taxonomic level.

The fungal unknown UF001 is shown in a Neighbor Joining phylogenetic tree with its ten closest genetic matches from GenBank (Figure 6). The taxa are colored to differentiate between the Lecanoromycete and Dothideomycete classes, and the fungal unknown is shown to nest within a clade that contains a Dothideomycete and another fungus of unknown class. All ten of the closest genetic matches belong to the subphylum Pezizomycotina, which makes it likely that UF001 also belongs to this subphylum, although its class is unable to be determined.

The fungal unknown UF002, which belongs to the order Chaetothyriales, is displayed in a phylogenetic tree with its ten closest genetic matches (Figure 7). It is nested in a clade that contains taxa from two different families, Trichomeriaceae and Herpotrichiellaceae. Its closest match on GenBank has a 99% sequence similarity but is of unknown genus. The next highest matches belong to the genera *Bradomyces* and *Coniosporium*, but these are of unknown species. Thus, higher taxonomic placement remains uncertain.

The fungal unknown UF003, which belongs to the family Saccharomycetaceae, is shown in a phylogenetic tree with its ten closest genetic matches (Figure 8). All taxa are colored blue to indicate that they belong to the *Candida* complex, despite different genus names for teleomorphs. UF003 has 100% sequence similarity to multiple taxa belonging to the *Candida* complex and can be considered *Candida sensu lato*.

The fungal unknown UF004, which belongs to the class Agaricomycetes, is shown in its phylogenetic tree nesting in a clade with taxa representing four different orders (Figure 9). The closest genetic match for the full 120 base pair sequence had 79% similarity in DNA sequence (Table 3). Thus, a taxonomic classification higher than class based on the ITS1 sequence is uncertain.

For the fungal unknown UF005, there were insufficient genetic matches on GenBank and the UNITE fungal database to construct a phylogenetic tree. The closest full-sequence match was an unidentified fungal sequence on the UNITE database belonging to the order Patellariales. This match had 98% sequence similarity to the UF005 sequence; however, that taxon remained unidentified past order. It is probable that UF005 also belongs to the order Patellariales due to its high similarity to the aforementioned taxon from the UNITE database.

The fungal unknown UF006, which belongs to the class Pezizomycetes, is shown in a phylogenetic tree with its ten most similar genetic matches from GenBank (Figure 10). Eight of the taxa in the tree belong to the family Pezizaceae, while two are of unknown family and are described as unclassified Pezizales. UF006 is most similar to taxa in the Pezizaceae family, while it is more distantly related to the unclassified taxa, Pezizales sp. P10 and Pezizales sp. SA233 (Figure 10). UF006 has a 98% sequence

similarity with all four strains of *Iodophanus testaceus*, and it is highly likely that UF006 belongs to the Pezizaceae family (Table 3).

The fungal unknown UF007, which belongs to the family Pezizaceae, is shown in a phylogenetic tree with its eight most similar genetic matches from GenBank (Figure 11). The closest genetic match from GenBank for the 120 base pair sequence had only a 78% similarity (Table 3). In Figure 11, the taxa belonging to the *Terfezia* genus form a monophyletic clade, while the taxa belonging to the *Peziza* genus are polyphyletic. UF007 does not nest within any clades in this tree. Any further taxonomic placement is highly uncertain based on the ITS1 sequence.

The fungal unknown UF008, which belongs to the family Mycosphaerellaceae, is shown in a phylogenetic tree with its ten most similar genetic matches from GenBank (Figure 12). This taxon has 100% sequence similarity with multiple genera, including *Acrodontium*, *Pseudocercospora*, and *Mycosphaerella*. Taxonomic classification beyond family is uncertain for UF008.

The last fungal unknown, UF009, belongs to the family Stachybotryaceae. Its placement in a phylogenetic tree along with its closest ten GenBank matches is shown in Figure 13. UF009 shared 100% sequence similarity with two taxa, *Alfaria terrestris* and *Myrothecium gramineum*. UF009 does not nest in any informative monophyletic clades. The *Alfaria*, *Myrothecium*, and *Amerosporium* genera in Figure 14 are all polyphyletic, and no genus forms a monophyletic clade. Taxonomic classification is uncertain for UF009 beyond family.

#### IV. DISCUSSION

The majority of fungal OTUs belonged to the phylum Ascomycota (forty-five OTUs), while the rest belonged to Basidiomycota (eight OTUs). These two phyla make up the vast majority of worldwide fungal taxa (Hawksworth 2001), so it is unsurprising to see such a representation here in this study. Many of the fungal species discovered are known to be associated with plants, either as epiphytes, endophytes, or pathogens. A full list of species along with their association with their hosts and substrates can be seen in in Table 2. Although many of these fungi primarily infect plants, they are not necessarily dependent on plants for the full life cycle. Thus, it is not surprising to find these species inside ant abdomens. It is uncertain whether these plant pathogens normally spend part of their life cycles inside arthropod hosts. Their occurrence could be due to the ants' consumption of infected plant parts. More research is needed to determine the role ants play in the fungal life cycles as well as the specificity between ant species and fungal species.

Although none of the taxa discovered are known to be pathogenic towards ants, it remains a possibility that a pathogenic relationship is yet to be discovered. *Penicillium corylophilum* is known to infect moths and mosquitoes (Lara da Costa et al. 1998; Thomazoni et al. 2014), while *Vishniacozyma heimaeyensis* (Basidionym: *Cryptococcus heimaeyensis*), has been found on insect larvae (Vishniac 2002). *V. heimaeyensis* has thus far only been isolated in Iceland, which makes its presence in the canopy of Amazonian Ecuador an exciting new discovery.

The genus with the most representation in this study is *Cladosporium*, an extremely common and widely distributed mold that typically infects plants.

*Cladosporium delicatulum* was identified from two sequence variants, and within this genus, it was also the species with the most abundance. This species is saprobic with a wide geographical range, and its spores are commonly found in high abundance in aerial samples (Bensch et al. 2010). Its presence in the ants is unsurprising due to its ubiquity in the air and throughout the world. *Cladosporium sp.* are known to cause allergic reactions in humans, although they are not considered of high medical significance (Flückiger et al. 2000). There were, however, other fungal species discovered in this study that have more significant medical implications.

Two species of *Penicillium*—a genus of fungi that produce medically significant compounds, the most important of which is penicillin—were observed in this study. *Penicillium corylophilum*, the first of these, is fairly widely distributed species that has been found growing as a mold in damp buildings (McMullin et al. 2014a) as well as living in the digestive tracts of many species of mosquitoes (Diptera: Culicidae) (Moraes et al. 2004). It is also pathogenic towards at least one species of moth, *Spodoptera frugiperda* (Thomazoni et al. 2014). *P. corylophilum* has been explored as a biocontrol agent for mosquito species that carry human tropical diseases (Lara da Costa et al. 1998). Additionally, its secondary metabolites have been shown to possess antimicrobial activity (Garcia Silva et al. 2004; McMullin et al. 2014b). Because these metabolites from Garcia Silva et al. 2004 differed greatly in their expression based on the growth media, it would be worthwhile to investigate the *in vivo* conditions of this fungal species as it pertains to tropical arboreal ants. Novel antibiotic applications could potentially result from studying how and why this fungus is associated with ants, as ants have been known to utilize microorganisms and their metabolites for antibacterial purposes (Currie et al. 1999).

The other species of *Penicillium* sequenced in this study is *P. bialowiezense*. This fungus has been isolated from soil as well as inside buildings in Canada; however, unlike *P. corylophilum*, this species is not known to be entomopathogenic (Scott et al. 2008). *P. bialowiezense* has not been researched as much as other *Penicillium* species, and it is uncertain if its presence in the canopy is due to the ants' diets, aquatic contamination, or entomopathogenicity.

Multiple fungi that are known to be human pathogens were discovered in this study. *Knufia epidermis*, known also as *Coniosporium epidermidis*, has recently been discovered in human skin lesions diagnosed as tinea nigra-like infections, and it is known to commonly exist asymptotically on human skin (Li et al. 2008). According to Li et al. 2008, this fungus was not just coincident in the skin lesions, as it penetrated all layers of the epidermis and basal membrane, and it was concluded that this species was the causative agent of infection. However, little is known regarding the environmental niches of *K. epidermidis* other than the human skin, and its presence here in ant abdomens in the canopy layer of the tropics is valuable in elucidating its ecological range and perhaps showing an intermediate host or vector.

Another human-pathogenic species, *Rhodotorula mucilaginosa*, is an opportunistic pathogenic yeast that has been isolated from human skin infections as well as from the blood stream when presenting as fungemia (Wirth and Goldani 2012). This yeast was detected in only one ant specimen, DPB001, in which it had the second highest abundance of the six total fungi detected for that ant. *Kodamaea ohmeri* has been found in human blood infections as well (Al-Sweih et al. 2011), while *Toxicocladosporium irritans* has been implicated in atopic dermatitis (eczema) cases (Zhang et al. 2011).

Other fungi in this study have been associated with skin diseases. *Coniochaeta polymorpha* is associated with neonatal throat infections (Khan et al. 2013), while *Cystobasidium slooffiae* (also known as *Malassezia slooffiae*) has been discovered to cause infections in both humans and goats (Uzal et al. 2007). More study is needed to determine whether arthropods can be vectors of any of these human- or mammal-pathogenic diseases or if they can be infected themselves.

The presence of multiple fungi known to infect humans has important conservation and ecological implications. With the rise in deforestation and resource extraction, especially in tropical areas, increasingly disturbing habitats in which these pathogenic fungi exist could potentially lead to increased human disease occurrence. As a few of the fungi discovered are known to cause human and livestock disease, it is important to adopt strategies for mitigating the deforestation in the Amazon as well as prevent the potential spread of diseases.

The relative abundances of the fungal sequences can show patterns in the distribution of certain genera and species, although the exact distribution of OTUs for each ant can be biased. Because there was an initial enrichment step to amplify flanking DNA regions, amplification bias was introduced. Some OTUs could be overrepresented due to the nested protocol, while others could be underrepresented or omitted entirely. Because of this, the relative abundances can only be considered loose approximations of the true relative abundances in nature. Additionally, DNA degradation is likely to have occurred for these specimens, which leads to an underrepresentation of diversity and abundance. The ant DNA was too degraded to amplify the cytochrome oxidase I gene,

which makes it likely that some fungal DNA was degraded as well. Although DNA degradation likely occurred, sufficient fungal DNA was amplified to identify most OTUs.

The multiple fungi that were unable to be identified taxonomically bolster the idea that the neotropics, the canopy layer, and bromeliads all deserve more study. One such fungus, labeled UF007 (Table 3) for which the closest known genetic match only shared 78% of identical base pairs, shows the massive gaps in knowledge there are for this ecological niche. Other unidentified fungi shared 100% ITS1 sequence similarity with multiple other genera or species for the 120 base pair sequences, which made it impossible to identify without morphological study. Future studies would benefit from using multiple barcoding loci in addition to culturing and morphological identification.

Although phylogenetic trees were constructed for the unidentified sequences, they are not informative in terms of evolutionary placement of these taxa. The ITS region is small, non-coding, and hypervariable, all of which make it a poor target for phylogenetic analyses. The value in constructing phylogenetic trees, particularly Neighbor Joining ones, is that they make a good visual representation of the relatedness of the closest genetic matches. With distance-based methods like Neighbor Joining, the branches are proportional to nucleotide differences among the taxa, which leads to an easily understood visual representation of genetic distance for multiple taxa. The topologies can be useful for determining the clades in which unknown fungi nest, but the trees are only as useful as the input sequences. With unidentified fungal taxa that are significantly different from known fungal sequences, such as UF007 (Table 3; Figure 11) the trees are less informative than those of highly similar fungal taxa, such as UF003 (Table 3; Figure 8).

This study underscores the importance of more research on fungal microbiomes, the canopy layer, and neotropical rainforests. Additionally, it sheds light on the possible reservoir of human and plant diseases in the canopy layer of the Amazonian rainforest, which is threatened by human encroachment. Despite the low sample size of this study, many unsequenced or uncultured fungi were discovered, and some of these fungal taxa show extreme sequence dissimilarity with their closest genetic matches. With greater sampling effort and advancements in high throughput parallel sequencing technologies, this vast untapped niche will likely see an abundance of discoveries in the near future.

**Table 1.** List of all fifty-three fungal OTUs and their highest levels of taxonomic classification along with the ant specimens to which they belong. P: phylum; C: class; O: order; F: family; G: genus; S: species

OTUs	Known Taxonomy	Ant IDs
OTU 01	<i>Alternaria</i> (G)	DPB002, DPB007, DPB020, DPB029, DPB041, DPB061, DPB080, DPB082, DPB096, DPB112, DPB129, DPB131, DPB144, DPB027
OTU 02	<i>Aspergillus restrictus</i> (S)	DPB027
OTU 03	<i>Aureobasidium pullulans</i> (S)	DPB001, DPB007, DPB020, DPB114
OTU 04	<i>Bipolaris</i> (G)	DPB065, DPB076
OTU 05	<i>Cladosporium sphaerospermum</i> (S)	DPB094
OTU 06	<i>Cladosporium</i> (G)	DPB038, DPB142
OTU 07	<i>Cladosporium delicatulum</i> (S)	DPB075
OTU 08	<i>Cladosporium</i> (G)	DPB089, DPB113, DPB116
OTU 09	<i>Cladosporium delicatulum</i> (S)	DPB030
OTU 10	<i>Cladosporium halotolerans</i> (S)	DPB143
OTU 11	<i>Coniochaeta polymorpha</i> (S)	DPB084
OTU 12	<i>Coniothrium glycines</i> (S)	DPB112
OTU 13	<i>Curvularia</i> (G)	DPB155
OTU 14	<i>Daldinia starbaeckii</i> (S)	DPB010
OTU 15	<i>Didymella</i> (G)	DPB091
OTU 16	<i>Epicoccum nigrum</i> (S)	DPB093
OTU 17	<i>Fusarium</i> (G)	DPB043, DPB127
OTU 18	<i>Fusarium</i> (G)	DPB074
OTU 19	<i>Knufia epidermidis</i> (S)	DPB056
OTU 20	<i>Kodamaea ohmeri</i> (S)	DPB061
OTU 21	<i>Meyerozyma guilliermondii</i> (S)	DPB077
OTU 22	<i>Mycosphaerella tassiana</i> (S)	DPB072
OTU 23	<i>Mycosphaerella tassiana</i> (S)	DPB015
OTU 24	<i>Mycosphaerella tassiana</i> (S)	DPB070
OTU 25	Ascomycota (P)	DPB109
OTU 26	Chaetothyriales (O)	DPB065
OTU 27	Saccharomycetaceae (F)	DPB101
OTU 28	Patellariales (O)	DPB002
OTU 29	Pezizomycetes (C)	DPB038
OTU 30	Pezizaceae (F)	DPB043
OTU 31	Mycosphaerellaceae (F)	DPB082
OTU 32	Stachybotryaceae (F)	DPB061, DPB116
OTU 33	<i>Nigrospora oryzae</i> (S)	DPB129
OTU 34	<i>Penicillium corylophilum</i> (S)	DPB057
OTU 35	<i>Penicillium bialowiezense</i> (S)	DPB109
OTU 36	<i>Periconia</i> (G)	DPB092

**Table 1. Continued.**

<b>OTUs</b>	<b>Known Taxonomy</b>	<b>Ant IDs</b>
OTU 37	<i>Pithomyces chartarum</i> (S)	DPB099
OTU 38	<i>Ramularia</i> (G)	DPB027
OTU 39	<i>Ramularia</i> (G)	DPB001, DPB002, DPB007, DPB096, DPB108, DPB131, DPB144
OTU 40	<i>Ramularia pratensis</i> (S)	DPB002
OTU 41	<i>Saccharomyces</i> (G)	DPB099
OTU 42	<i>Saccharomyces</i> (G)	DPB108
OTU 43	<i>Talaromyces ruber</i> (S)	DPB001
OTU 44	<i>Toxicocladosporium irritans</i> (S)	DPB061
OTU 45	<i>Yarrowia lipolytica</i> (S)	DPB001
OTU 46	<i>Cystobasidium slooffiae</i> (S)	DPB002, DPB116
OTU 47	<i>Cystoflobasidium infirmominiatum</i> (S)	DPB035
OTU 48	Agaricomycetes (C)	DPB072
OTU 49	<i>Phlebiopsis gigantea</i> (S)	DPB112
OTU 50	<i>Pleurotus abieticola</i> (S)	DPB089
OTU 51	<i>Rhodotorula mucilaginosa</i> (S)	DPB001
OTU 52	<i>Vishniacozyma</i> (G)	DPB061
OTU 53	<i>Vishniacozyma heimaeyensis</i> (S)	DPB101

**Table 2.** List of all fungal species and genera, their known hosts or substrates, and the relationship to their hosts or substrates.

<b>Fungal Taxon</b>	<b>Substrate</b>	<b>Relation to Substrate</b>
<i>Alternaria sp.</i>	Soil, decomposing wood	Saprobic
<i>Aspergillus restrictus</i>	House dust, soil, plant leaves	Saprobic, Pathogenic
<i>Aureobasidium pullulans</i>	Plant leaves	Mutualistic
<i>Bipolaris sp.</i>	Plant leaves	Pathogenic
<i>Cladosporium delicatulum</i>	Plant-pathogenic fungi	Pathogenic
<i>Cladosporium halotolerans</i>	Saltwater, indoor swabs, soil, humans	Saprobic, Pathogenic
<i>Cladosporium sp.</i>	Soil, plant leaves, aerial samples	Saprobic, Pathogenic
<i>Cladosporium sphaerospermum</i>	Indoor swabs, dolphins	Saprobic
<i>Coniochaeta polymorpha</i>	Plant leaves, human neonatal throats	Pathogenic
<i>Coniothyrium glycines</i>	Plant leaves	Pathogenic
<i>Curvularia sp.</i>	Plant leaves	Pathogenic
<i>Cystobasidium slooffiae</i>	Human throats	Pathogenic
<i>Cystofilobasidium infirmominiatum</i>	Apple and citrus fruit surface	Mutualistic
<i>Daldinia starbaeckii</i>	Decaying wood	Saprobic
<i>Didymella sp.</i>	Plant stems	Pathogenic
<i>Epicoccum nigrum</i>	Plant leaves	Pathogenic
<i>Fusarium sp.</i>	Plant leaves	Pathogenic
<i>Knufia epidermidis</i>	Human foot infection	Pathogenic
<i>Kodamaea ohmeri</i>	Human yeast infection, blood infection	Pathogenic
<i>Meyerozyma guilliermondii</i>	Human skin	Pathogenic
<i>Mycosphaerella tassiana</i>	Plant leaves	Pathogenic
<i>Nigrospora oryzae</i>	Plant leaves	Pathogenic
<i>Penicillium bialowiezense</i>	Indoor mold, soil	Saprobic
<i>Penicillium corylophilum</i>	Mosquitoes, indoor mold	Saprobic, Pathogenic
<i>Periconia sp.</i>	Soil, Plants	Saprobic
<i>Phlebiopsis gigantea</i>	Decaying conifers	Saprobic
<i>Pithomyces chartarum</i>	Plant leaves	Pathogenic
<i>Pleurotus abieticola</i>	Decaying wood	Saprobic
<i>Ramularia pratensis</i>	Plant leaves	Pathogenic
<i>Ramularia sp.</i>	Plant leaves	Pathogenic
<i>Rhodotorula mucilaginosa</i>	Human yeast infection	Pathogenic
<i>Saccharomyces sp.</i>	Soil, plant surfaces	Saprobic
<i>Talaromyces ruber</i>	Plant leaves	Pathogenic
<i>Toxicocladosporium irritans</i>	Human skin, indoor mold, plant surfaces	Saprobic, Pathogenic
<i>Vishniacozyma heimaeyensis</i>	Soil, insect larvae	Saprobic
<i>Vishniacozyma sp.</i>	Soil	Saprobic
<i>Yarrowia lipolytica</i>	High-oil substrates	Saprobic

**Table 3.** All unknown OTUs along with their highest level of taxonomic classification, their likely next level of taxonomic classification, and the match percentage of the closest genetic sequence of known fungal species with full coverage on GenBank and UNITE fungal databases. P: Phylum; SP: Subphylum; C: Class; O: Order; F: Family; G: Genus.

<b>Unknown ID</b>	<b>Known Taxonomy</b>	<b>Likely Taxonomy</b>	<b>Highest Match %</b>
UF001	Ascomycota (P)	Pezizomycotina (SP)	83
UF002	Chaetothyriales (O)	Uncertain	98
UF003	Saccharomycetaceae (F)	<i>Candida</i> (G)	100
UF004	Agaricomycetes (C)	Uncertain	79
UF005	Patellariales (O)	Uncertain	98
UF006	Pezizomycetes (C)	Pezizaceae (F)	98
UF007	Pezizaceae (F)	Uncertain	78
UF008	Mycosphaerellaceae (F)	Uncertain	100
UF009	Stachybotryaceae (F)	Uncertain	100

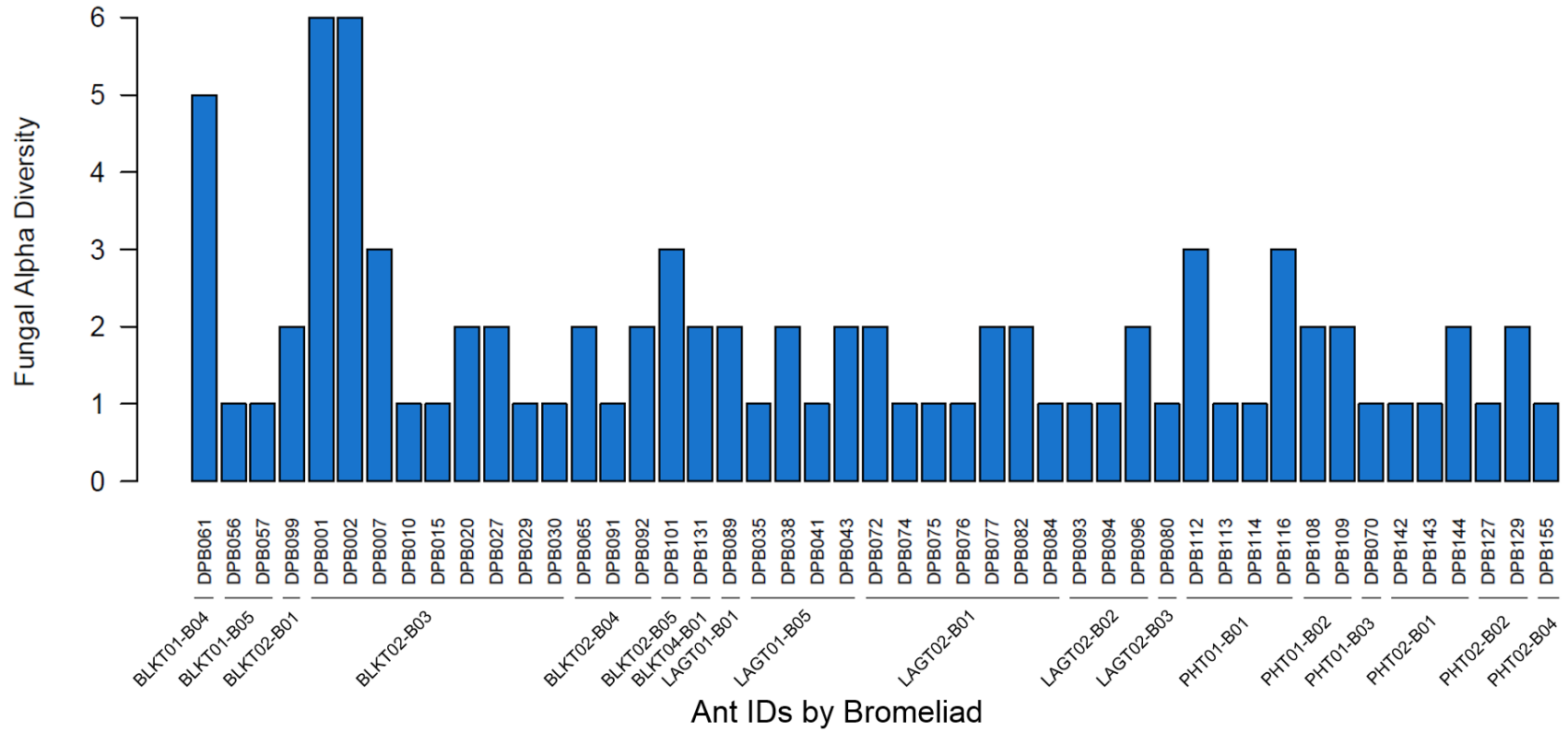


**Figure 1. Alpha diversity plot.** Total observed unique fungal species for 47 ant specimens and their associated bromeliads.

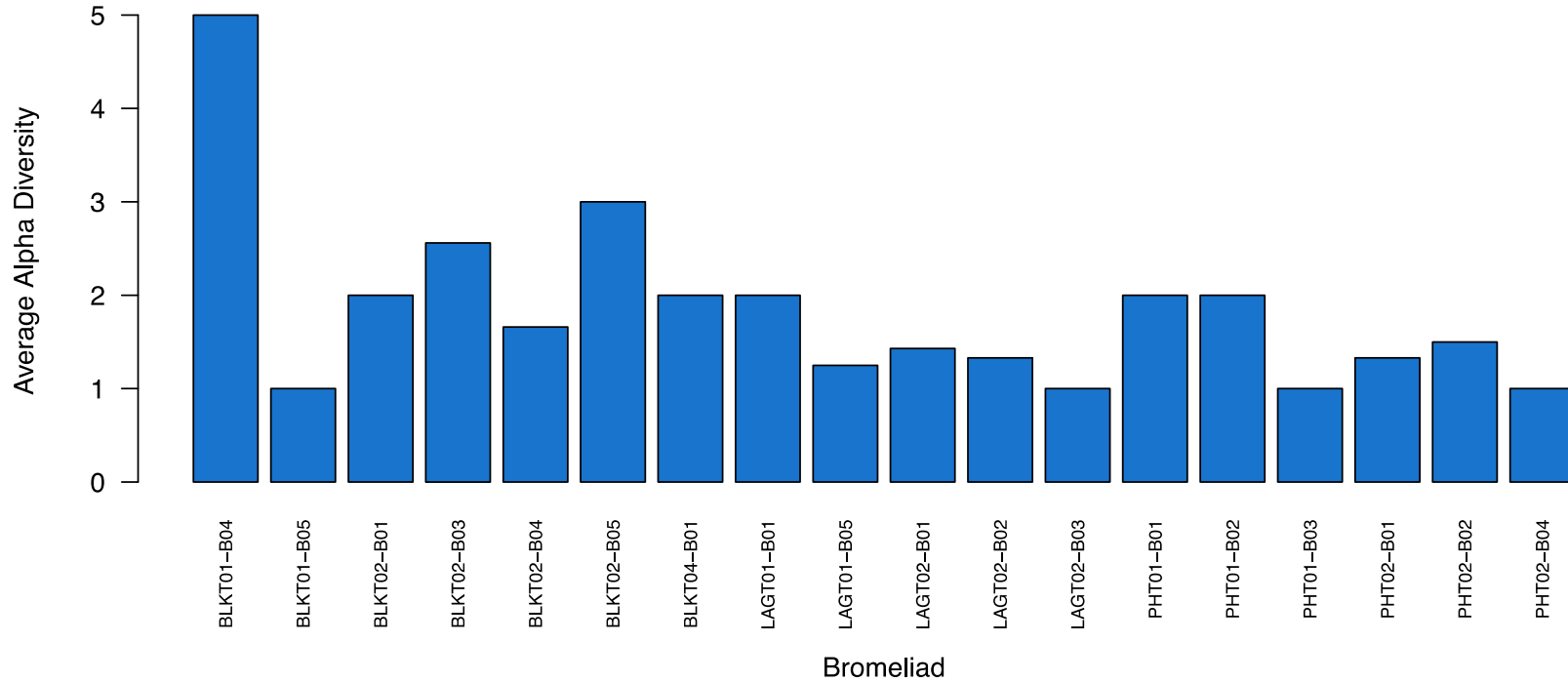


**Figure 2. Average alpha diversity plot per bromeliad.** The average fungal alpha diversity for ants within each bromeliad is plotted. The first three letters denote location within the study area; the first two numbers denote the tree number within the location; the last two numbers denote the bromeliad on the given tree.

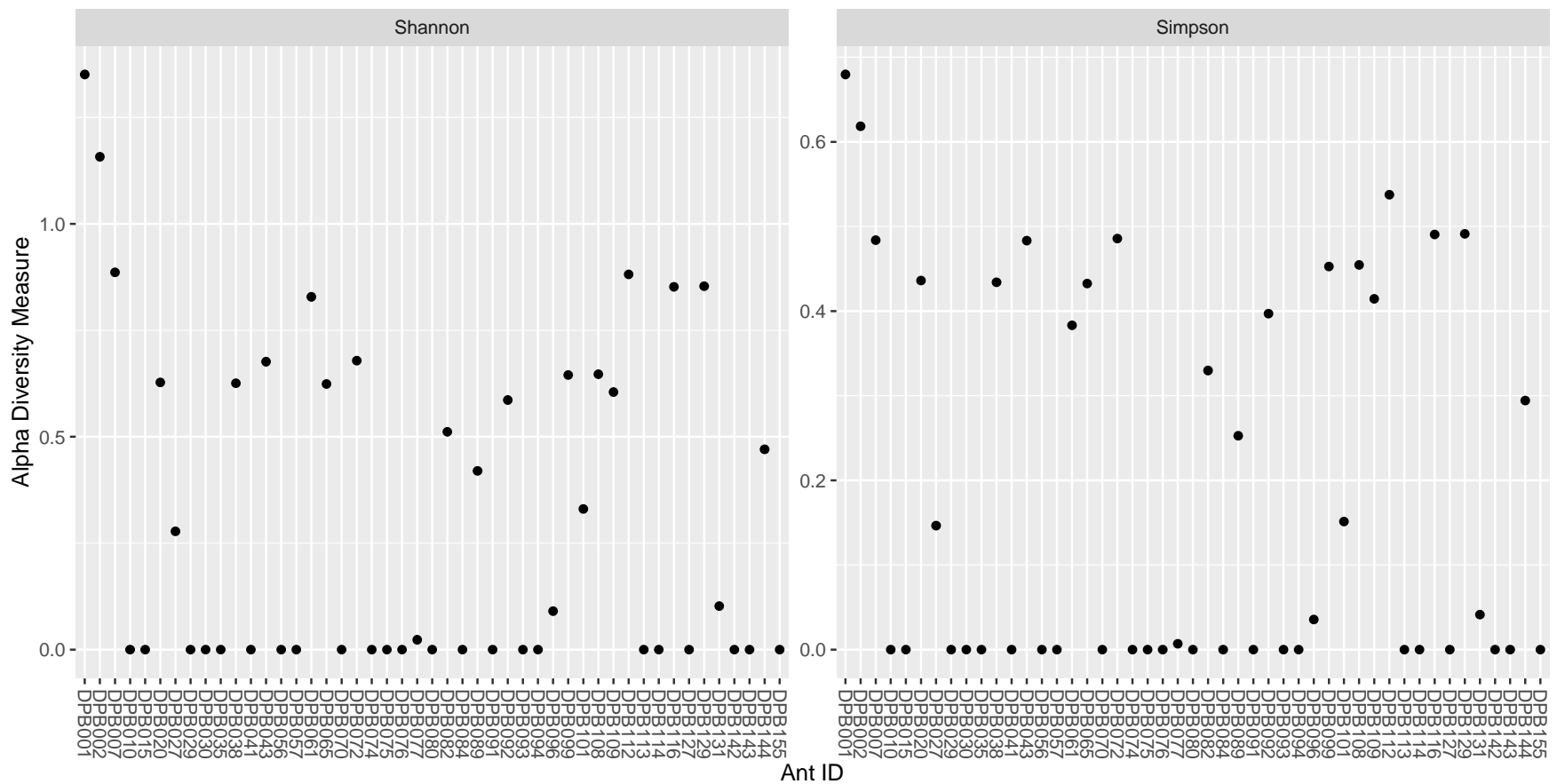


**Figure 3. Shannon-Wiener and Simpson diversity plot.** Plot showing the Shannon-Wiener and Simpson diversity measures for all fungal OTUs for each of the 47 ant specimens.

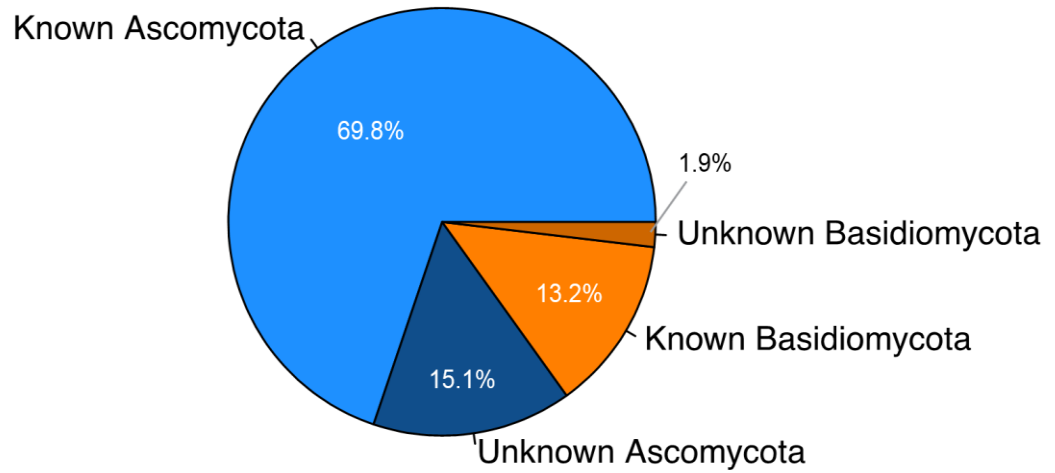


**Figure 4. Pie chart of phyla.** Represents the phyla of all fifty-three discrete fungal OTUs found, proportional by unique sequence variants. The unknowns refer to fungal sequences that were unable to be identified to genus.

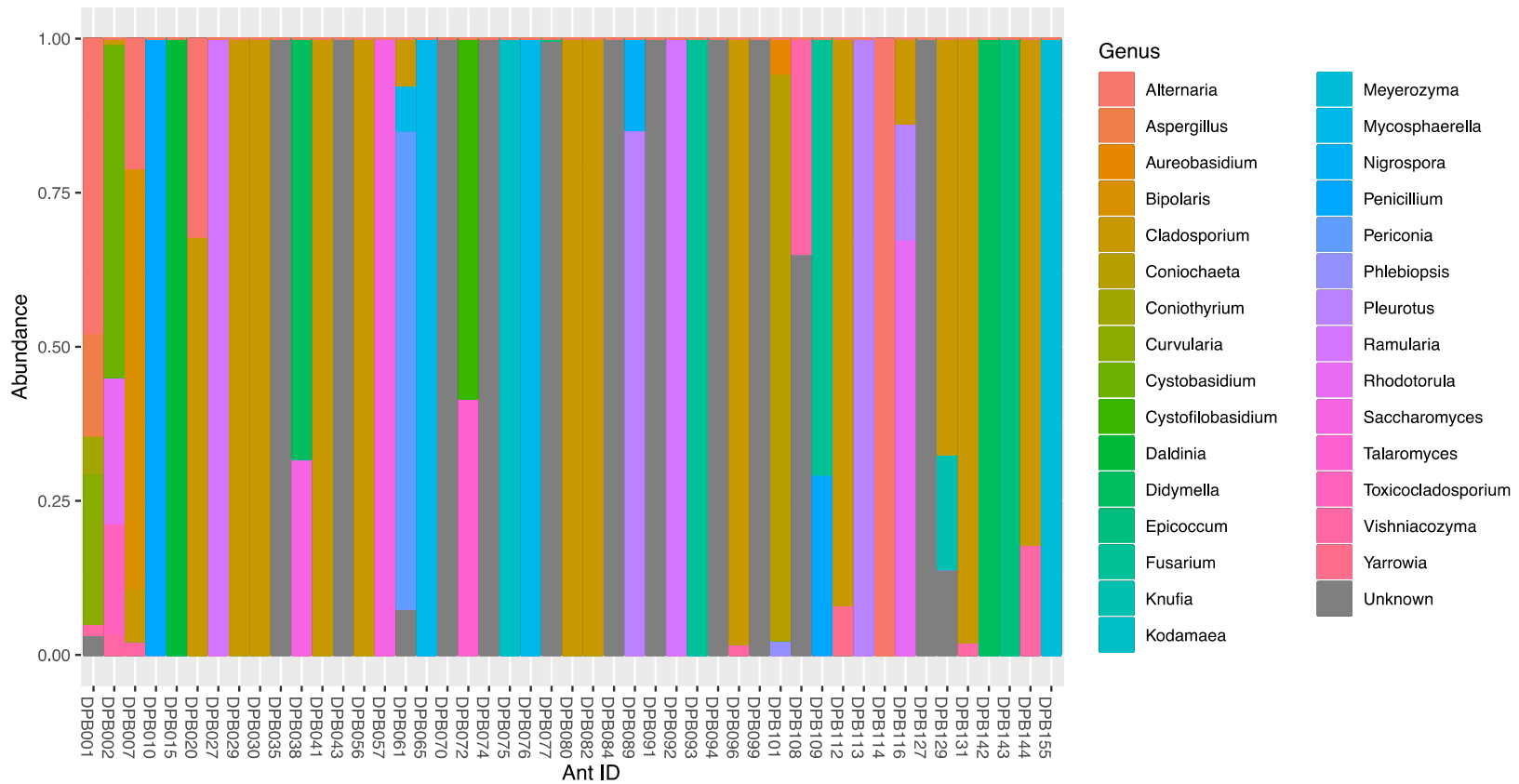


**Figure 5. Stacked bar plot of relative fungal abundance.** Shows the fungal genera represented for each ant specimen, proportional to fungal sequence read numbers. Sequence variants unable to be identified to genus level are denoted by “Unknown” in the legend.

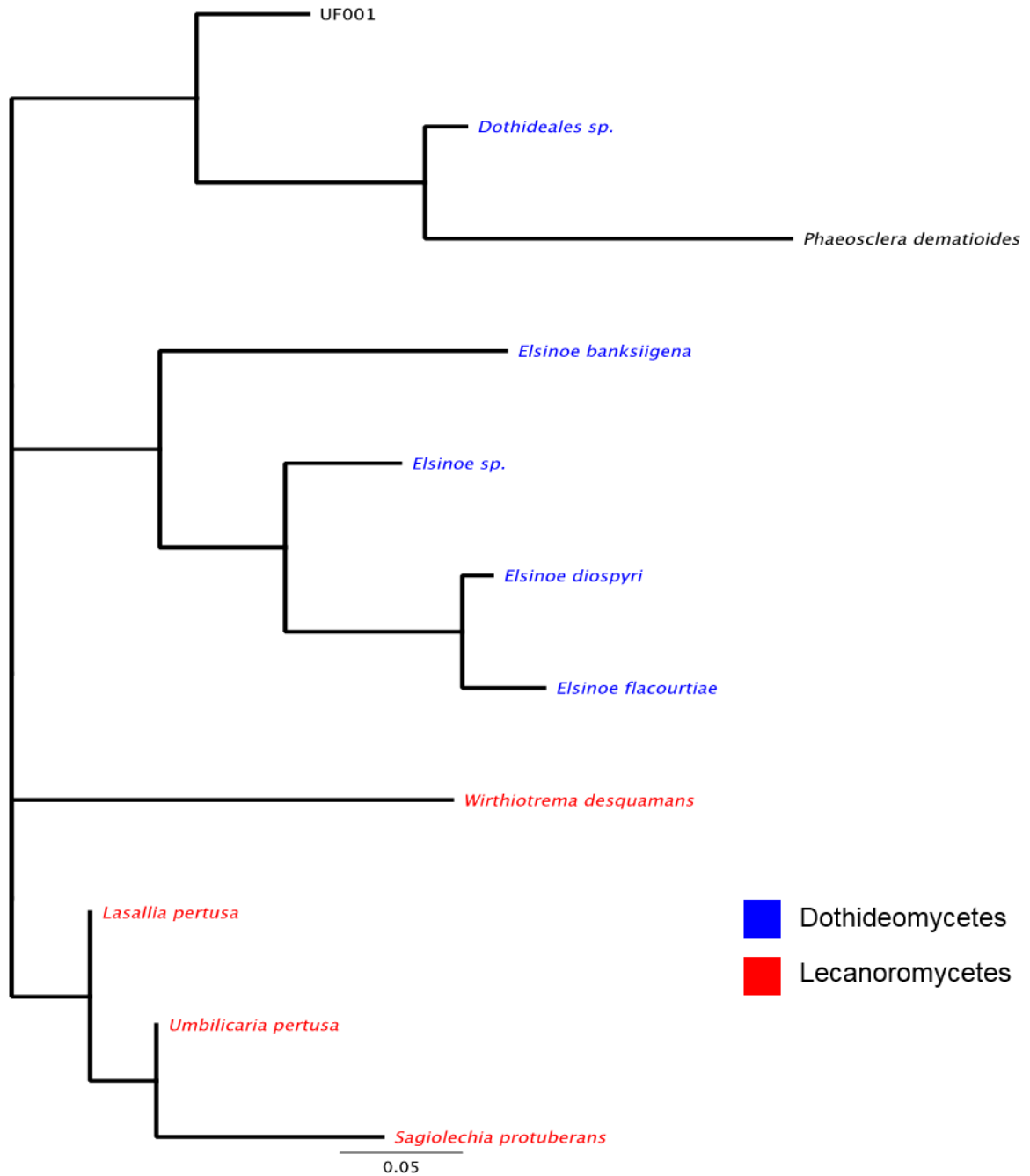


**Figure 6. Phylogeny of UF001.** Unrooted Neighbor Joining phylogenetic tree using a 120 base pair alignment of the ten closest ITS1 sequence matches to UF001 on GenBank, generated in Geneious 9.1.8 with the GTR+I+G nucleotide model. Scale indicating substitutions per site shown at bottom. Blue taxa: Dothideomycetes; red taxa: class Lecanoromycetes; black: unknown class.

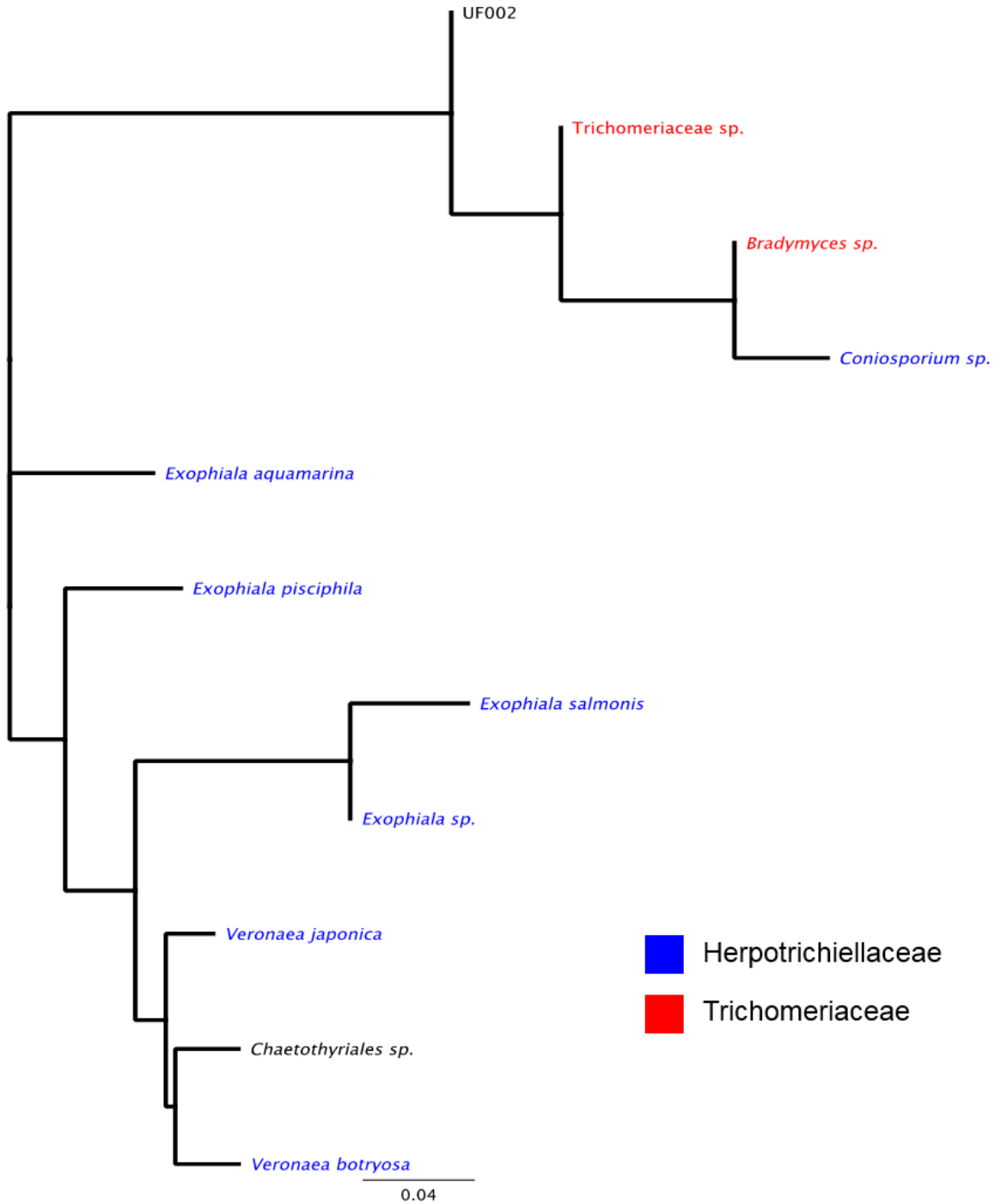


**Figure 7. Phylogeny of UF002.** Unrooted Neighbor Joining phylogenetic tree using a 120 base pair alignment of the ten closest ITS1 sequence matches to UF002 on GenBank, generated in Geneious 9.1.8 with the GTR+I+G nucleotide model. Scale indicating substitutions per site shown at bottom.

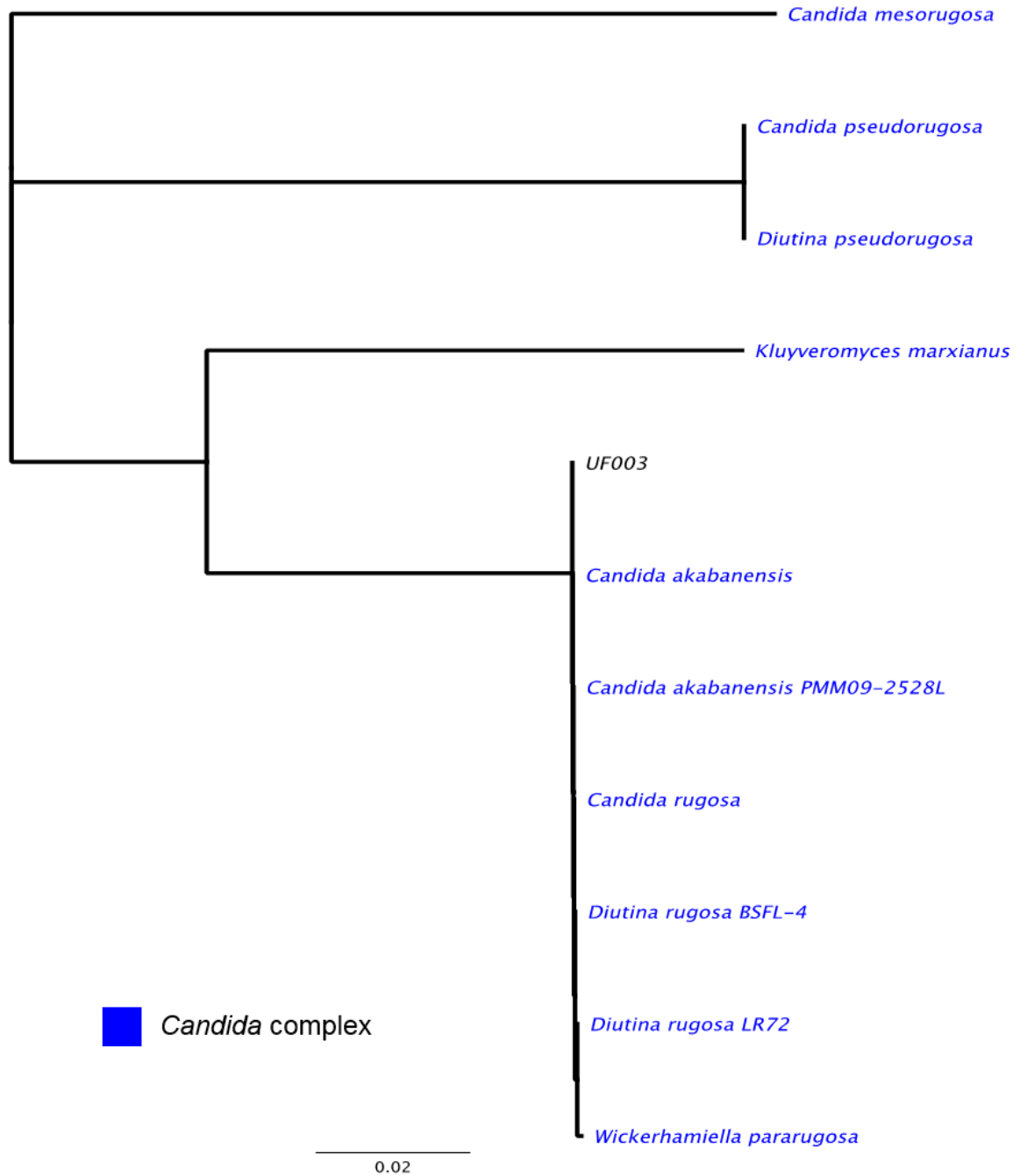


**Figure 8. Phylogeny of UF003.** Unrooted Neighbor Joining phylogenetic tree using a 120 base pair alignment of the ten closest ITS1 sequence matches to UF003 on GenBank, generated in Geneious 9.1.8 with the GTR+I+G nucleotide model. Scale indicating substitutions per site shown at bottom.

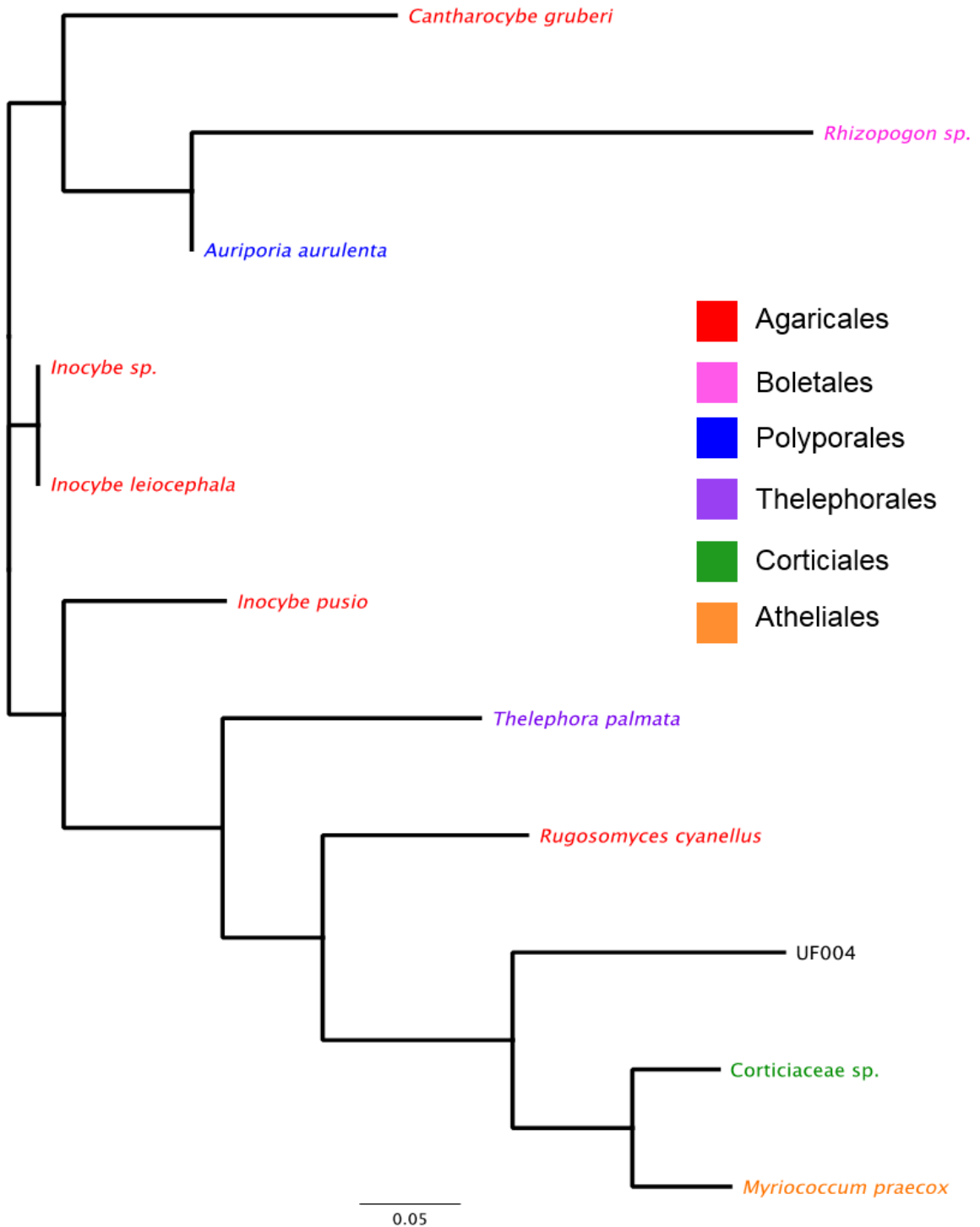


**Figure 9. Phylogeny of UF004.** Unrooted Neighbor Joining phylogenetic tree using a 120 base pair alignment of the ten closest ITS1 sequence matches to UF004 on GenBank, generated in Geneious 9.1.8 with the GTR+I+G nucleotide model. Scale indicating substitutions per site shown at bottom.

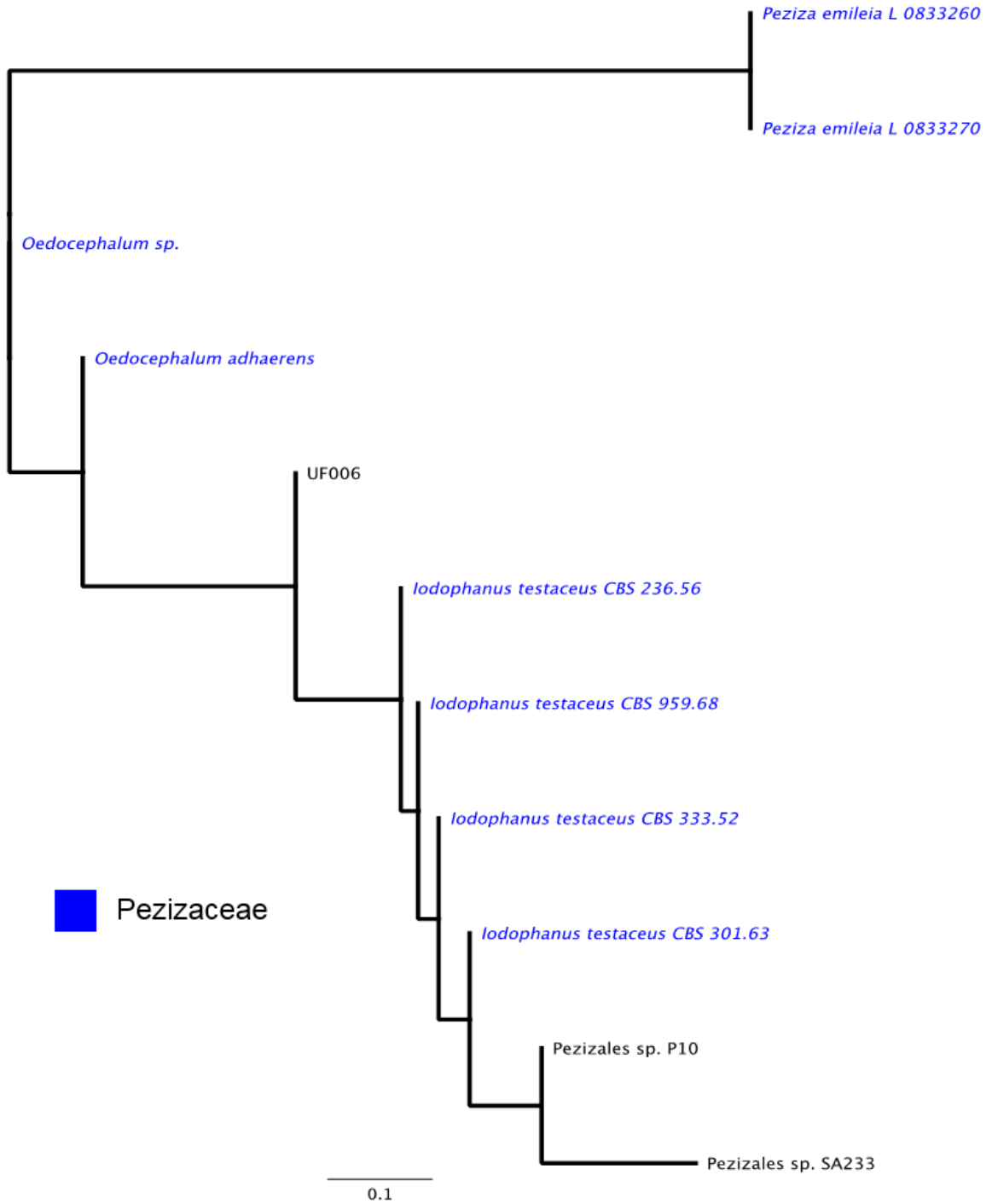


**Figure 10. Phylogeny of UF006.** Unrooted Neighbor Joining phylogenetic tree using a 120 base pair alignment of the ten closest ITS1 sequence matches to UF006 on GenBank, generated in Geneious 9.1.8 with the GTR+I+G nucleotide model. Scale indicating substitutions per site shown at bottom.

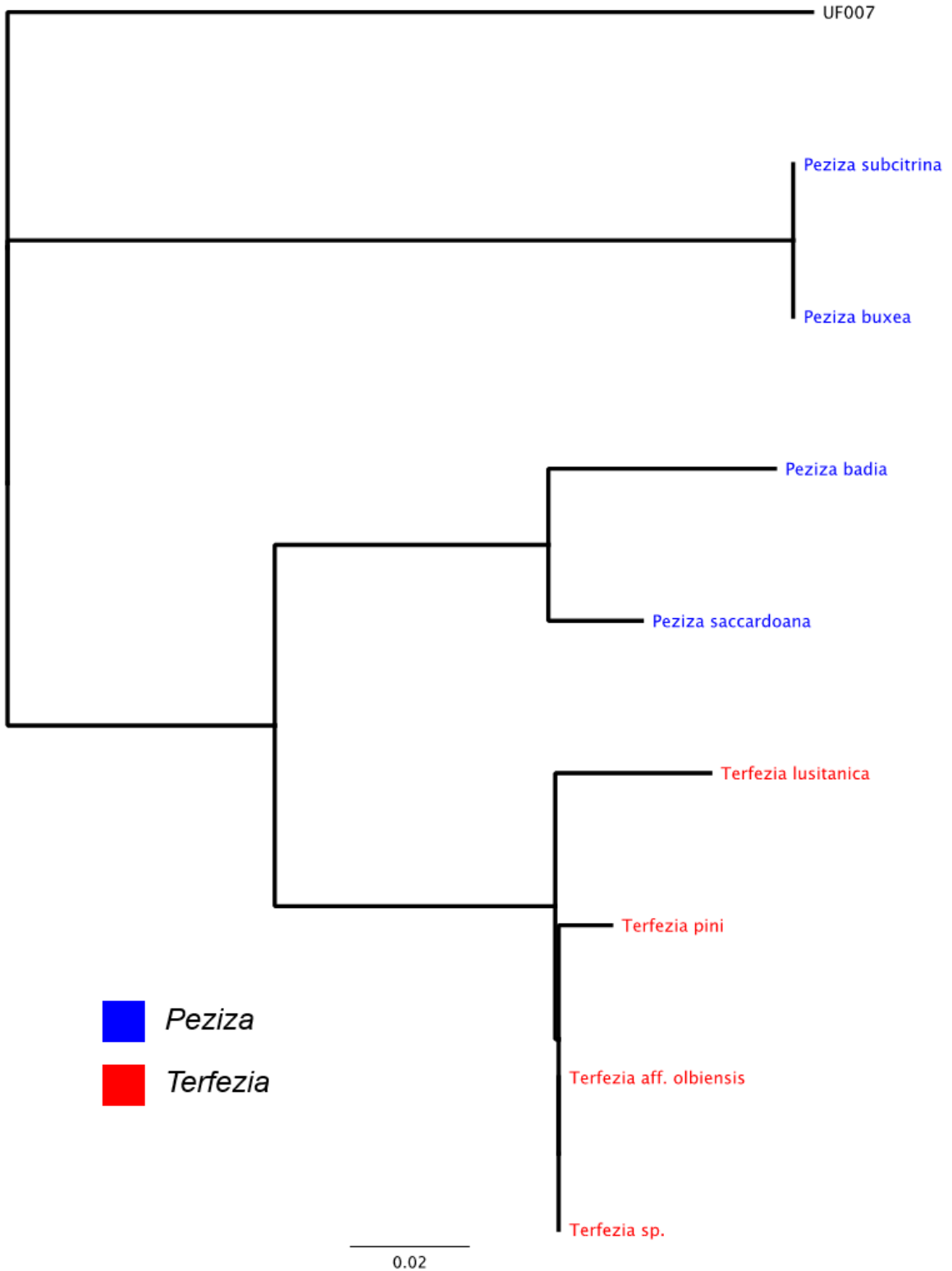


**Figure 11. Phylogeny of UF007.** Unrooted Neighbor Joining phylogenetic tree using a 120 base pair alignment of the eight closest ITS1 sequence matches to UF007 on GenBank, generated in Geneious 9.1.8 with the GTR+I+G nucleotide model. Scale indicating substitutions per site shown at bottom.

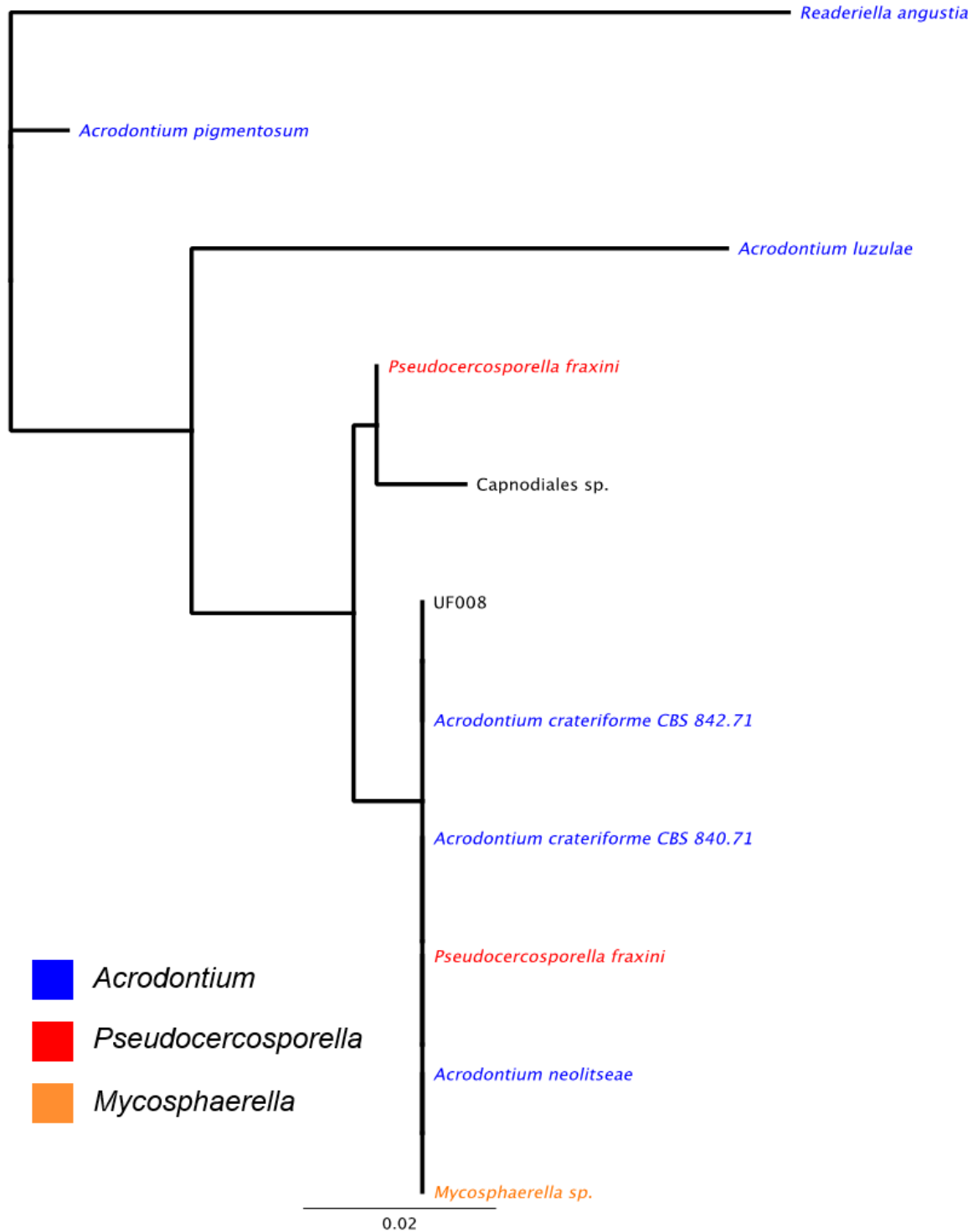


**Figure 12. Phylogeny of UF008.** Unrooted Neighbor Joining phylogenetic tree using a 120 base pair alignment of the ten closest ITS1 sequence matches to UF008 on GenBank, generated in Geneious 9.1.8 with the GTR+I+G nucleotide model. Scale indicating substitutions per site shown at bottom.

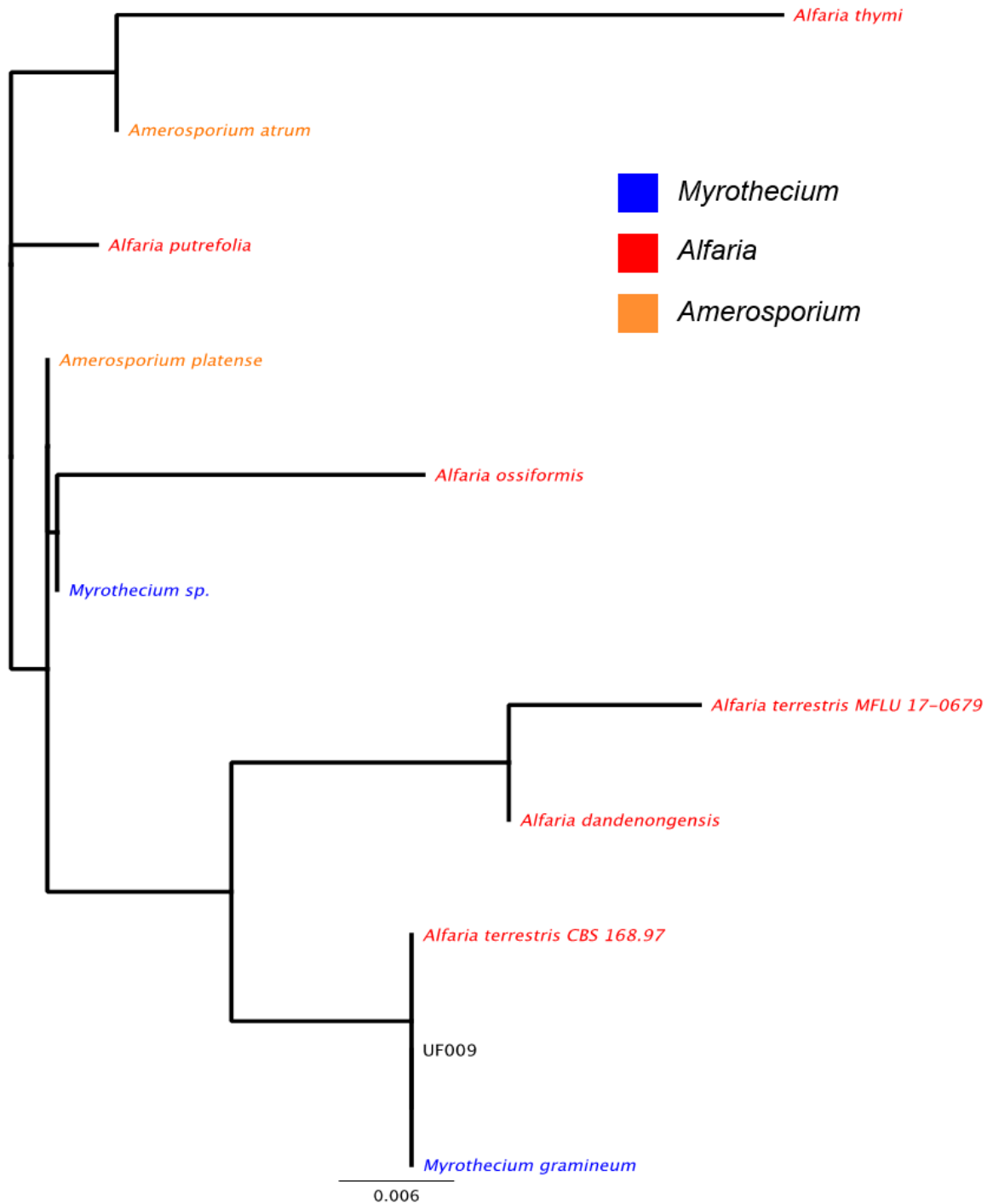


**Figure 13. Phylogeny of UF009.** Unrooted Neighbor Joining phylogenetic tree using a 120 base pair alignment of the ten closest ITS1 sequence matches to UF009 on GenBank, generated in Geneious 9.1.8 with the GTR+I+G nucleotide model. Scale indicating substitutions per site shown at bottom.

## APPENDIX SECTION

**Appendix A.** ID: ant identification number; BRM: bromeliad; A: total anurans; DT: date; LAT: latitude; LON: longitude; ALT: altitude (m); DBH: tree diameter at breast height (cm); HT: tree height (m); CT: bromeliad count; CC: canopy cover (%); EV: bromeliad elevation (m); BH: bromeliad height (cm); BD: bromeliad diameter (cm); BL: bromeliad leaf count; BV: bromeliad water volume (mL); BT: bromeliad temperature (°C); SPH: soil pH; SM: soil moisture (%); WPH: water pH; PHP: water pH (post); ND: no data

ID	BRM	A	DT	LAT	LON	ALT	DBH	HT	CT	CC	EV	BH	BD	BL	BV	BT	SPH	SM	WPH	PHP
DPB001	BLKT02-B03	1	27-Jul-06	-0.63461	-76.18410	233.7	100.9	45	25	93.24	28.7	75	57	41	3645	29.5	5.7	0.75	5.04	5.03
DPB002	BLKT02-B03	1	27-Jul-06	-0.63461	-76.18410	233.7	100.9	45	25	93.24	28.7	75	57	41	3645	29.5	5.7	0.75	5.04	5.03
DPB007	BLKT02-B03	1	27-Jul-06	-0.63461	-76.18410	233.7	100.9	45	25	93.24	28.7	75	57	41	3645	29.5	5.7	0.75	5.04	5.03
DPB010	BLKT02-B03	1	27-Jul-06	-0.63461	-76.18410	233.7	100.9	45	25	93.24	28.7	75	57	41	3645	29.5	5.7	0.75	5.04	5.03
DPB015	BLKT02-B03	1	27-Jul-06	-0.63461	-76.18410	233.7	100.9	45	25	93.24	28.7	75	57	41	3645	29.5	5.7	0.75	5.04	5.03
DPB020	BLKT02-B03	1	27-Jul-06	-0.63461	-76.18410	233.7	100.9	45	25	93.24	28.7	75	57	41	3645	29.5	5.7	0.75	5.04	5.03
DPB027	BLKT02-B03	1	27-Jul-06	-0.63461	-76.18410	233.7	100.9	45	25	93.24	28.7	75	57	41	3645	29.5	5.7	0.75	5.04	5.03
DPB029	BLKT02-B03	1	27-Jul-06	-0.63461	-76.18410	233.7	100.9	45	25	93.24	28.7	75	57	41	3645	29.5	5.7	0.75	5.04	5.03
DPB030	BLKT02-B03	1	27-Jul-06	-0.63461	-76.18410	233.7	100.9	45	25	93.24	28.7	75	57	41	3645	29.5	5.7	0.75	5.04	5.03
DPB035	LAGT01-B05	2	10-Aug-06	-0.63839	-76.15383	222.8	132.1	39	75	91.94	33.61	112	112	24	1566	28.5	5.1	0.61	4.22	4.55
DPB038	LAGT01-B05	2	10-Aug-06	-0.63839	-76.15383	222.8	132.1	39	75	91.94	33.61	112	112	24	1566	28.5	5.1	0.61	4.22	4.55
DPB041	LAGT01-B05	2	10-Aug-06	-0.63839	-76.15383	222.8	132.1	39	75	91.94	33.61	112	112	24	1566	28.5	5.1	0.61	4.22	4.55
DPB043	LAGT01-B05	2	10-Aug-06	-0.63839	-76.15383	222.8	132.1	39	75	91.94	33.61	112	112	24	1566	28.5	5.1	0.61	4.22	4.55
DPB056	BLKT01-B05	4	20-Jul-06	-0.63536	-76.18390	220	114.6	48.5	150	93.24	35.2	86	72	22	1670	26.5	5.8	0.6	5.39	4.63
DPB057	BLKT01-B05	4	20-Jul-06	-0.63536	-76.18390	220	114.6	48.5	150	93.24	35.2	86	72	22	1670	26.5	5.8	0.6	5.39	4.63
DPB061	BLKT01-B04	0	20-Jul-06	-0.63536	-76.18390	220	114.6	48.5	150	93.24	34.5	73	102	22	868	26.5	5.8	0.6	5.04	4.74
DPB065	BLKT02-B04	0	27-Jul-06	-0.63461	-76.18410	233.7	100.9	45	25	93.24	29.48	77	91	27	1270	30	5.7	0.75	5.22	4.82
DPB070	PHT01-B03	0	13-Jul-06	-0.64330	-76.14050	213.5	131.5	50.5	35	ND	32.36	68	107	22	503	26	6.3	0.68	ND	4.7
DPB072	LAGT02-B01	1	13-Aug-06	-0.63966	-76.15393	205.6	63.4	28	34	90.38	22.49	87	55	37	2644	31	5.4	0.75	4.72	4.41
DPB074	LAGT02-B01	1	13-Aug-06	-0.63966	-76.15393	205.6	63.4	28	34	90.38	22.49	87	55	37	2644	31	5.4	0.75	4.72	4.41
DPB075	LAGT02-B01	1	13-Aug-06	-0.63966	-76.15393	205.6	63.4	28	34	90.38	22.49	87	55	37	2644	31	5.4	0.75	4.72	4.41
DPB076	LAGT02-B01	1	13-Aug-06	-0.63966	-76.15393	205.6	63.4	28	34	90.38	22.49	87	55	37	2644	31	5.4	0.75	4.72	4.41
DPB077	LAGT02-B01	1	13-Aug-06	-0.63966	-76.15393	205.6	63.4	28	34	90.38	22.49	87	55	37	2644	31	5.4	0.75	4.72	4.41
DPB080	LAGT02-B03	1	13-Aug-06	-0.63966	-76.15393	205.6	63.4	28	34	90.38	20.52	73	71	25	1595	31	5.4	0.75	4.52	4.98
DPB082	LAGT02-B01	1	13-Aug-06	-0.63966	-76.15393	205.6	63.4	28	34	90.38	22.49	87	55	37	2644	31	5.4	0.75	4.72	4.41
DPB084	LAGT02-B01	1	13-Aug-06	-0.63966	-76.15393	205.6	63.4	28	34	90.38	22.49	87	55	37	2644	31	5.4	0.75	4.72	4.41
DPB089	LAGT01-B01	0	10-Aug-06	-0.63839	-76.15383	222.8	132.1	39	75	91.94	27.7	94	94	17	42*	27.5	5.1	0.61	3.89	4.27
DPB091	BLKT02-B04	0	27-Jul-06	-0.63461	-76.18410	233.7	100.9	45	25	93.24	29.48	77	91	27	1270	30	5.7	0.75	5.22	4.82
DPB092	BLKT02-B04	0	27-Jul-06	-0.63461	-76.18410	233.7	100.9	45	25	93.24	29.48	77	91	27	1270	30	5.7	0.75	5.22	4.82
DPB093	LAGT02-B02	1	13-Aug-06	-0.63966	-76.15393	205.6	63.4	28	34	90.38	21.21	83	101	29	1650	31	5.4	0.75	4.49	4.36
DPB094	LAGT02-B02	1	13-Aug-06	-0.63966	-76.15393	205.6	63.4	28	34	90.38	21.21	83	101	29	1650	31	5.4	0.75	4.49	4.36
DPB096	LAGT02-B02	1	13-Aug-06	-0.63966	-76.15393	205.6	63.4	28	34	90.38	21.21	83	101	29	1650	31	5.4	0.75	4.49	4.36
DPB099	BLKT02-B01	0	27-Jul-06	-0.63461	-76.18410	233.7	100.9	45	25	93.24	27.8	79	104	20	580	31	5.7	0.75	4.53	4.97
DPB101	BLKT02-B05	0	27-Jul-06	-0.63461	-76.18410	233.7	100.9	45	25	93.24	30.4	73	62	23	647	31	5.7	0.75	4.38	5.04
DPB108	PHT01-B02	0	13-Jul-06	-0.64330	-76.14050	213.5	131.5	50.5	35	ND	31.75	67	106	26	355	26	6.3	0.68	ND	4.71
DPB109	PHT01-B02	0	13-Jul-06	-0.64330	-76.14050	213.5	131.5	50.5	35	ND	31.75	67	106	26	355	26	6.3	0.68	ND	4.71
DPB112	PHT01-B01	0	13-Jul-06	-0.64330	-76.14050	213.5	131.5	50.5	35	ND	30.48	65	99	23	130	27	6.3	0.68	ND	4.32
DPB113	PHT01-B01	0	13-Jul-06	-0.64330	-76.14050	213.5	131.5	50.5	35	ND	30.48	65	99	23	130	27	6.3	0.68	ND	4.32
DPB114	PHT01-B01	0	13-Jul-06	-0.64330	-76.14050	213.5	131.5	50.5	35	ND	30.48	65	99	23	130	27	6.3	0.68	ND	4.32
DPB116	PHT01-B01	0	13-Jul-06	-0.64330	-76.14050	213.5	131.5	50.5	35	ND	30.48	65	99	23	130	27	6.3	0.68	ND	4.32
DPB127	PHT02-B02	0	17-Jul-06	-0.64431	-76.13925	220.1	64	37	100	88.3	23.7	585	670	19	704	27	6.0	0.62	4.84	4.13
DPB129	PHT02-B02	0	17-Jul-06	-0.64431	-76.13925	220.1	64	37	100	88.3	23.7	585	670	19	704	27	6.0	0.62	4.84	4.13
DPB131	BLKT04-B01	4	4-Aug-06	-0.63649	-76.18246	222.6	116.2	46	42	94.28	29.55	74	148	32	457	29.5	5.2	0.75	6.34	4.45
DPB142	PHT02-B01	0	17-Jul-06	-0.64431	-76.13925	220.1	64	37	100	88.3	22.4	85	85	23	940	28.5	6.0	0.62	6.61	4.35
DPB143	PHT02-B01	0	17-Jul-06	-0.64431	-76.13925	220.1	64	37	100	88.3	22.4	85	85	23	940	28.5	6.0	0.62	6.61	4.35
DPB144	PHT02-B01	0	17-Jul-06	-0.64431	-76.13925	220.1	64	37	100	88.3	22.4	85	85	23	940	28.5	6.0	0.62	6.61	4.35
DPB155	PHT02-B04	0	17-Jul-06	-0.64431	-76.13925	220.1	64	37	100	88.3	24.8	740	670	18	1480	27.5	6.0	0.62	4.36	4.24

## LITERATURE CITED

- Al-Sweih N., Khan Z.U., Ahmad S., Devarajan L., Khan S., Joseph L., Chandy R. 2011. *Kodamaea ohmeri* as an emerging pathogen: a case report and review of the literature. *Med. Mycol.* 49:1–5.
- Bensch K., Groenewald J.Z., Dijksterhuis J., Starink-Willemse M., Andersen B., Summerell B.A., Shin H.-D., Dugan F.M., Schroers H.-J., Braun U., Crous P.W. 2010. Species and ecological diversity within the *Cladosporium cladosporioides* complex (Davidiellaceae, Capnodiales). *Stud. Mycol.* 67:1–94.
- Buée M., Reich M., Murat C., Morin E., Nilsson R.H., Uroz S., Martin F. 2009. 454 Pyrosequencing analyses of forest soils reveal an unexpectedly high fungal diversity. *New Phytol.* 184:449–456.
- Currie C.R., Scott J.A., Summerbell R.C., Malloch D. 1999. Erratum: Fungus-growing ants use antibiotic-producing bacteria to control garden parasites. *Nature.* 398:701–704.
- Dowd P.F. 1992. Insect fungal symbionts: A promising source of detoxifying enzymes. *J. Ind. Microbiol.* 9:149–161.
- Evans H.C., Elliot S.L., Hughes D.P. 2011. *Ophiocordyceps unilateralis*: A keystone species for unraveling ecosystem functioning and biodiversity of fungi in tropical forests? *Commun. Integr. Biol.* 4:598–602.
- Flückiger B., Koller T., Monn C. 2000. Comparison of airborne spore concentrations and fungal allergen content. *Aerobiologia (Bologna).* 16:393.

- Garcia Silva M., Araçari Jacometti Cardoso Furtado N., Tallarico Pupo M., José Vieira Fonseca M., Said S., Alves da Silva Filho A., Kenupp Bastos J. 2004. Antibacterial activity from *Penicillium corylophilum* Dierckx. *Microbiol. Res.* 159:317–322.
- Gloor G.B., Hummelen R., Macklaim J.M., Dickson R.J., Fernandes A.D., MacPhee R., Reid G. 2010. Microbiome Profiling by Illumina Sequencing of Combinatorial Sequence-Tagged PCR Products. *PLoS One.* 5:e15406.
- Hawksworth D.L. 2001. The magnitude of fungal diversity: the 1.5 million species estimate revisited. *Mycol. Res.* 105:1422–1432.
- Hawksworth D.L., Lücking R. 2017. Fungal Diversity Revisited: 2.2 to 3.8 Million Species. *The Fungal Kingdom.* American Society of Microbiology. p. 79–95.
- Hebert P.D.N., Gregory T.R., Savolainen V. 2005. The Promise of DNA Barcoding for Taxonomy. *Syst. Biol.* 54:852–859.
- Hoog G.S., Ende A.H.G.G. 1998. Molecular diagnostics of clinical strains of filamentous Basidiomycetes. *Mycoses.* 41:183–189.
- Khan Z., Gené J., Ahmad S., Cano J., Al-Sweih N., Joseph L., Chandy R., Guarro J. 2013. *Coniochaeta polymorpha*, a new species from endotracheal aspirate of a preterm neonate, and transfer of *Lecythophora* species to *Coniochaeta*. *Antonie Van Leeuwenhoek.* 104:243–252.

- Kõljalg U., Nilsson R.H., Abarenkov K., Tedersoo L., Taylor A.F.S., Bahram M., Bates S.T., Bruns T.D., Bengtsson-Palme J., Callaghan T.M., Douglas B., Drenkhan T., Eberhardt U., Dueñas M., Grebenc T., Griffith G.W., Hartmann M., Kirk P.M., Kohout P., Larsson E., Lindahl B.D., Lücking R., Martín M.P., Matheny P.B., Nguyen N.H., Niskanen T., Oja J., Peay K.G., Peintner U., Peterson M., Põldmaa K., Saag L., Saar I., Schüßler A., Scott J.A., Senés C., Smith M.E., Suija A., Taylor D.L., Telleria M.T., Weiss M., Larsson K.-H. 2013. Towards a unified paradigm for sequence-based identification of fungi. *Mol. Ecol.* 22:5271–5277.
- Lara da Costa G., Lage de Moraes A.M., Cunha de Oliveira P. 1998. Pathogenic action of *Penicillium* species on mosquito vectors of human tropical diseases. *J. Basic Microbiol.* 38:337–341.
- Li D.M., de Hoog G.S., Saunte D.M.L., van den Ende A.H.G.G., Chen X.R. 2008. *Coniosporium epidermidis* sp. nov., a new species from human skin. *Stud. Mycol.* 61:131–6.
- Liu K.-L., Porrás-Alfaro A., Kuske C.R., Eichorst S.A., Xie G. 2012. Accurate, rapid taxonomic classification of fungal large-subunit rRNA genes. *Appl. Environ. Microbiol.* 78:1523–33.
- Lowman M.D., Schowalter T.D. 2012. Plant science in forest canopies - the first 30 years of advances and challenges (1980-2010). *New Phytol.* 194:12–27.
- Mardis E.R. 2008. The impact of next-generation sequencing technology on genetics. *Trends Genet.* 24:133–41.

- McMullin D.R., Nsiama T.K., Miller J.D. 2014a. Secondary metabolites from *Penicillium corylophilum* isolated from damp buildings. *Mycologia*. 106:621–628.
- McMullin D.R., Nsiama T.K., Miller J.D. 2014b. Isochromans and  $\alpha$ -Pyrones from *Penicillium corylophilum*. *J. Nat. Prod.* 77:206–212.
- Moraes A.M.L. de, Junqueira A.C.V., Celano V., Costa G.L. da, Coura J.R. 2004. Fungal flora of the digestive tract of *Rhodnius prolixus*, *Rhodnius neglectus*, *Diptelanogaster maximus* and *Panstrongylus megistus*, vectors of *Trypanosoma cruzi*, Chagas, 1909. *Brazilian J. Microbiol.* 35:288–291.
- Moran V.C., Southwood T.R.E. 1982. The Guild Composition of Arthropod Communities in Trees. *J. Anim. Ecol.* 51:289.
- Moritz C., Cicero C. 2004. DNA Barcoding: Promise and Pitfalls. *PLoS Biol.* 2:e354.
- Mullis K.B., Faloona F.A. 1987. [21] Specific synthesis of DNA in vitro via a polymerase-catalyzed chain reaction. *Methods Enzymol.* 155:335–350.
- Nadkarni N.M. 1994. Diversity of Species and Interactions in the Upper Tree Canopy of Forest Ecosystems. *Am. Zool.* 34:70–78.
- Quail M.A., Kozarewa I., Smith F., Scally A., Stephens P.J., Durbin R., Swerdlow H., Turner D.J. 2008. A large genome center's improvements to the Illumina sequencing system. *Nat. Methods.* 5:1005–1010.

- Schoch C.L., Seifert K.A., Huhndorf S., Robert V., Spouge J.L., Levesque C.A., Chen W., Fungal Barcoding Consortium F.B. 2012. Nuclear ribosomal internal transcribed spacer (ITS) region as a universal DNA barcode marker for Fungi. *Proc. Natl. Acad. Sci. U. S. A.* 109:6241–6.
- Scott J.A., Wong B., Summerbell R.C., Untereiner W.A. 2008. A survey of *Penicillium brevicompactum* and *P. bialowiezense* from indoor environments, with commentary on the taxonomy of the *P. brevicompactum* group. *Botany.* 86:732–741.
- Smith D.R., Quinlan A.R., Peckham H.E., Makowsky K., Tao W., Woolf B., Shen L., Donahue W.F., Tusneem N., Stromberg M.P., Stewart D.A., Zhang L., Ranade S.S., Warner J.B., Lee C.C., Coleman B.E., Zhang Z., McLaughlin S.F., Malek J.A., Sorenson J.M., Blanchard A.P., Chapman J., Hillman D., Chen F., Rokhsar D.S., McKernan K.J., Jeffries T.W., Marth G.T., Richardson P.M. 2008. Rapid whole-genome mutational profiling using next-generation sequencing technologies. *Genome Res.* 18:1638–42.
- Stuntz S., Ziegler C., Simon U., Zotz G. 2002. Diversity and structure of the arthropod fauna within three canopy epiphyte species in central Panama. *J. Trop. Ecol.* 18:161–176.

Tedersoo L., Bahram M., Polme S., Koljalg U., Yorou N.S., Wijesundera R., Ruiz L. V., Vasco-Palacios A.M., Thu P.Q., Suija A., Smith M.E., Sharp C., Saluveer E., Saitta A., Rosas M., Riit T., Ratkowsky D., Pritsch K., Poldmaa K., Piepenbring M., Phosri C., Peterson M., Parts K., Partel K., Otsing E., Nouhra E., Njouonkou A.L., Nilsson R.H., Morgado L.N., Mayor J., May T.W., Majuakim L., Lodge D.J., Lee S.S., Larsson K.-H., Kohout P., Hosaka K., Hiiesalu I., Henkel T.W., Harend H., Guo L. -d., Greslebin A., Grelet G., Geml J., Gates G., Dunstan W., Dunk C., Drenkhan R., Dearnaley J., De Kesel A., Dang T., Chen X., Buegger F., Brearley F.Q., Bonito G., Anslan S., Abell S., Abarenkov K. 2014. Global diversity and geography of soil fungi. *Science*. 346:1256688.

Thomazoni D., Formentini M.A., Alves L.F.A. 2014. Patogenicidade de isolados de fungos entomopatogênicos à *Spodoptera frugiperda* (Smith) (Lepidoptera: Noctuidae). *Arq. Inst. Biol. (Sao. Paulo)*. 81:126–133.

Uzal F.A., Paulson D., Eigenheer A.L., Walker R.L. 2007. *Malassezia slooffiae*-associated dermatitis in a goat. *Vet. Dermatol.* 18:348–352.

Vishniac H.S. 2002. *Cryptococcus tephrensis*, sp.nov., and *Cryptococcus heimaeyensis*, sp.nov.; new anamorphic basidiomycetous yeast species from Iceland. *Can. J. Microbiol.* 48:463–467.

White T., Bruns T., Lee S., Taylor J. 1990. Amplification and direct sequencing of fungal ribosomal RNA genes for phylogenetics. In: Innis M., Gelfand D., Shinsky J., White T., editors. *PCR Protocols: A Guide to Methods and Applications*. San Diego: Academic Press. p. 315–322.

Wirth F., Goldani L.Z. 2012. Epidemiology of *Rhodotorula*: an emerging pathogen.

Interdiscip. Perspect. Infect. Dis. 2012:465717.

Zhang E., Tanaka T., Tajima M., Tsuboi R., Nishikawa A., Sugita T. 2011.

Characterization of the skin fungal microbiota in patients with atopic dermatitis and in healthy subjects. Microbiol. Immunol. 55:625–632.